THE EFFECT OF INBOUND MASS ON THE DYNAMIC RESPONSE OF THE HYBRID III HEADFORM AND BRAIN TISSUE DEFORMATION.

Clara Karton

Advisor
Thomas Blaine Hoshizaki, PhD

Committee
Gordon Robertson, PhD
Jingxian Li, PhD

November, 2012

School of Human Kinetics
Faculty of Health Science
University of Ottawa

ABSTRACT

The varied impact parameters that characterize an impact to the head have shown to influence the resulting type and severity of outcome injury, both in terms of the dynamic response, and the corresponding deformation of neural tissue. Therefore, when determining head injury risks through event reconstruction, it is important to understand how individual impact characteristics influence these responses. The effect of inbound mass had not yet been documented in the literature. The purpose of this study was to determine the effects of inbound mass on the dynamic impact response and brain tissue deformation. A 50^{th} percentile Hybrid III adult male head form was impacted using a simple pendulum system. Impacts to a centric and a non-centric impact location were performed with six varied inbound masses at a velocity of 4.0 m/s. The peak linear and peak angular accelerations were measured. A finite element model, (UCDBTM) was used to determine brain deformation, namely peak maximum principal strain and peak von Mises stress. Inbound mass produced significant differences for peak linear acceleration for centric ($F(5, 24) = 217.55$, $p=.0005$) and non-centric ($F(5, 24) = 161.98$, $p=.0005$), and for peak angular acceleration for centric ($F(5, 24) = 52.51$, $p=.0005$) and non-centric ($F(5, 24) = 4.18$, $p=.007$) impact locations. A change in inbound mass also had a significant effect on peak maximum principal strain for centric ($F(5, 24) = 11.04$, $p=.0005$) and non-centric ($F(5, 24) = 5.87$, $p =.001$), and for peak von Mises stress for centric ($F(5, 24) = 24.01$, $p=.0005$) and non-centric ($F(5, 24) = 4.62$, $p=.004$) impact locations. These results indicate the inbound mass of an impact should be of consideration when determining risks and prevention to head and brain injury.

ACKNOWLEDGEMENTS

I would like to take this opportunity to thank my research supervisor, Dr. Thomas Blaine Hoshizaki, for providing me with guidance and encouragement throughout the completion of this thesis. His enthusiastic attitude and endless passion that he displays towards his work has been a true inspiration and a pleasure to have experienced. In addition, I would like to extend this thank you to the members of my committee, Dr. Gordon Robertson and Dr. Jingxian Li, for offering their expertise in providing important and challenging questions. Finally, I would like to recognize the lab coordinator Andrew Post, and my colleagues and personnel of the Neurotrauma Impact Science Laboratory Philippe Rousseau, Marshall Kendall, Anna Oeur, and Evan Walsh for their persistent assistance and teaching.

TABLE OF CONTENTS

LIST OF FIGURES

LIST OF TABLES

CHAPTER 1. INTRODUCTION

1.1 PROBLEM STATEMENT

Concussions, or mild traumatic brain injuries (mTBI), are common injuries seen in recreational and professional sports even when using protective headgear (Delaney, Lacroix, Leclerc & Johnston, 2002; Zazryn et al., 2006). In efforts to decrease the incidence of mTBI, it is important to understand the mechanisms relating to these injuries, and the resulting neural tissue damage. Not all head impacts are the same and as a result differ in a number of characteristics including impact site, mass, velocity, angle of impact and compliance of impactor, creating unique dynamic and head responses and consequently different head and brain injuries (Gennarelli et al., 1982; 1987; Zhang, Yang & King, 2001; Kleiven, 2003, Pellman, Viano, Tucker & Casson, 2003). In order to decrease the incidence and risks of head injuries, it is necessary that the mechanism by which these brain injuries occur be better understood. Furthermore, when attempting to establish the risks of brain injury, understanding the dynamic response of the head under different impact conditions is important.

Force can be calculated using the product of mass and acceleration, therefore as the force of the impact increases, it would be expected that the resulting acceleration experienced by the head of a given mass would also increase proportionally (Barth, Freeman, Broshek & Varney, 2001), and consequently have an influence on the risk of injury (Newman, 2006). The impact of the head and helmet on an object is complex involving a number of materials all of different shapes and orientation effecting the relationship between force, mass and acceleration. The mass and acceleration of an object is only one part of the characteristics affecting the dynamic response of the head. The moment of inertia of the objects, the

material characteristics of the head and object it is hitting as well as the geometry of the impact surfaces all effect the equation.

Protective headgear, or helmets are designed to attenuate impact energy by decreasing the magnitude of force of the impact. However, research has yet to establish the influence of inbound mass, in altering the force of the impact and subsequently the dynamic response of the head. Finally the resulting dynamic effect of the head will predict the magnitude of force on the brain tissue (Barth et al., 2001). Impact reconstruction employing physical models and finite element analysis has become an important tool for examining the effects that varying impact conditions have on the resulting dynamic response of the head, and the corresponding deformation of neural tissue (Willinger & Baumgarthner, 2003; Zhang, Yang, King & Viano, 2003; 2004). Understanding the effects that these impact conditions have on the dynamic response of the head and tissue stress of the brain will provide insight into the effect these variables play in the accuracy of methodologies when undertaking research and interpreting results for injury mechanisms.

1.2 OVERVIEW

With the advent of helmet standards in sports, Traumatic Brain Injuries (TBI) have decreased dramatically (Bailes & Cantu, 2001). However the incidence of mild traumatic brain injury (mTBI), have not and continue to be a concern in both recreational and professional sports (Delaney et al., 2002; Flik, Lyman & Marc, 2005; Casson, Viano, Powell & Pellman, 2010). A recent survey indicated that 110 in 100,000 Canadians suffer from a concussion, or mild traumatic brain injury each year (Gordon, Dooley & Wood, 2006). Of the reported concussion, over 54% were sports-related incidences. Although these terms, concussion and mTBI are deemed one in the same, the severity of concussion injuries is broad, where symptoms and recovery times differ, and may not always be described as a ‘mild’ injury

(Meehan, 2011). Often post-concussion symptoms are used in the diagnosis and prognosis of concussion injuries, although symptoms and recovery time can differ dramatically between individuals (Iverson, Lange, Brooks & Rennison, 2010; Leclerc, Lassonde, Delaney, Lacroix & Johnston, 2001). Due to the wide -range of differences between individuals and how they respond to concussion injuries, a universal grading system does not exist and lacks experimental evidence (Leclerc et al. 2001). In 2011, Meaney and Smith reported that there are 225,000 new patients annually in the US that show long-term deficits from mTBI. To put this into perspective, this is approximately equal to the number of patients per year diagnosed with breast cancer, multiple sclerosis, and traumatic spinal cord injuries combined. This is indicative of how this injury is of a growing concern. A better understanding of the mechanisms and impact parameters that cause mTBI injuries will provide valuable insight into injury prevention and management of the risks associated with concussions.

The majority of helmet safety standards around the world primarily use centric testing protocols based solely on linear accelerations ranging from 250-300g as indicators of injury (Goldsmith & Plunkett, 2004). This resulted in successfully decreasing traumatic brain injuries, however they may not fully encompass and protect against the mechanisms for concussion (Bailes & Cantu, 2001). Linear acceleration shows poor correlation with angular acceleration and brain tissue deformation variables (King, Yang, Zhang & Hardy, 2003; Rousseau, Post & Hoshizaki, 2009; Walsh, Rousseau & Hoshizaki, 2011; Forero Rueda, Cui & Gilchrist, 2010), where both have been associated with mechanisms responsible for risks of mTBI (Holbourn, 1943; Gennarelli et al., 1982; Willinger & Baumgarthner, 2003; Zhang, et al., 2003; 2004; Kleiven, 2007).

An impact to the head is defined by a rapid onset of high forces over a short duration (Barth et al., 2001). According to Newman (2006) the severity of injury from an impact, is a direct result of the magnitude of the impacting force. Newton's Second Law of Motion describes the relationship between force, mass and acceleration. This law states that the resultant force is equal to the product of mass and acceleration ($\sum F = ma$). Peak linear acceleration is a vector quantity that describes the rate of change of linear velocity over time. Therefore given the same head mass, an impact would result in a higher acceleration with an increasing impacting force (Newman, 2006), and thus a more severe head injury. A force in newtons (N) is defined by the effect that one object or body will have upon another, where 1 N=1 $kg.m/s^2$ (Robertson, 1997). In other words, force is dependent on the moving objects mass, space, and time (Robertson, 1997).

During impacts in which the head or body is struck by or strikes a blunt object the force can be distributed over a broad area, and in these cases the impact energy can be absorbed by crushable material such as in helmet liners (Avalle, Belingardi, & Montanini, 2001). These forces have the ability to generate acceleration and deformation of the head and tissues, where both can be the cause of injury (Viano, King, Melvin & Weber, 1989; Kleiven & von Holst, 2002).

Helmets are designed to attenuate the impact energy or magnitude of the force, through deformable materials, thereby increasing the duration of an impact and reducing the linear acceleration experienced by the head, resulting in decrease of injury severity (Nahum, Smith & Ward, 1977; Kleiven & von Holst, 2002). The liner within the helmet is the primary energy-absorbing material (Hoshizaki & Brien, 2004), and is designed to function properly within a designated energy range. This means that the material will not be as effective at an inbound momentum (mass x velocity) that is either too high or too low (Avalle et al., 2001).

With any impact of a given energy, the resultant impulse experienced by the head will be the same, however the force-time curve shape will change depending if energy-absorbing material is present (Hodgson, 1967). The energy-absorbing material will increase the duration at which the force is fully transmitted, decreasing the magnitude of the force. Impacts in which a high force is experienced in a short duration can cause more serious injury, or material failure sooner, than those impacts where the force transmission is prolonged and dampened (Hodgson, 1967). However this force-time curve shape is not only dependent on the presence of a helmet, but also depends on the interaction of the striking object and, in this case the skull, brain, and surrounding soft tissues (Hodgson, 1967), and therefore may influence the peak accelerations experienced and thus the resulting head injury.

The resulting kinematic outputs from impacts to the head, such as linear and angular accelerations assume the head to be a rigid body, and therefore may not fully encompass the mechanisms behind these injuries. Brain tissue damage results from acceleration, however the acceleration itself is not the cause of injury. As the head undergoes a linear impact, the force causes the brain to move and strike the inner skull either in its initial direction, causing coup injury, or during the rebound where the brain strikes the inner skull in the opposite direction causing contrecoup injury (Barth et al., 2001). Moreover during rotation, the brain strikes the inner skull multiple times, and therefore could result in higher tissue alteration (Barth et al., 2001). This was demonstrated by King and colleagues (2003) who found that linear acceleration caused relative brain motion of one millimeter (±1 mm) compared to angular acceleration, which induced brain motion of as much as five millimeters (±5 mm). In efforts to understand the mechanisms of concussion, reconstruction of head injury is a widely used method for investigating the relationship between the event causing brain injury

and the resulting trauma to neural tissue (Willinger & Baumgarthner, 2003; Zhang, et al., 2003; 2004). The description of the impact unfortunately is usually limited to a 2 dimensional video or a verbal description (Willinger & Baumgarthner, 2003; Pellman et al., 2003; Viano & Pellman, 2005), consequently presenting possible errors in the impact parameters used to describe the event. Understanding the degree of which the impact characteristics influence the accuracy of the reconstruction is important when interpreting brain stress values obtained from reconstructions.

The use of physical models such as anthropomorphic test devices, dummies, and biofidelic head forms, are common to represent human physical properties for impact testing for protective headgear used in various sports, as well as in accident reconstruction methodologies (CAN/CSA-D113.2-M89, 1996; Snell Memorial Foundation, 2007; NOCSAE *001-06m07*, 2007; Willinger & Baumgarthner, 2003; Zhang, et al., 2003; 2004). These impacts are performed on surfaces that are designed to mimic the realistic impact scenarios (CAN/CSA-D113.2-M89, 1996; NOCSAE *001-06m07*, 2007). In addition, technological advancements have allowed for the development of finite element models of the human brain and skull to gain knowledge into the interaction and reaction of the brain tissue under impact (Kleiven & Hardy, 2002; Horgan & Gilchrist, 2003).

The interaction and compliance of the materials for both physical models, and finite element analysis may affect the force equation (Hodgson, 1967), and therefore the sensitivity of these methodologies is important to consider when establishing mechanisms of injury, brain deformation, and injury prevention from accident reconstructions. Moreover, the kinematic response of the head may not correlate with the response of the viscoelastic properties of the brain (Forero Rueda, et al., 2010) from a change in inbound mass, or force of impact. Therefore, examining both the dynamic response of the head and the tissue response under

varying impact conditions helps to better understand the relationship between the mechanisms of injury and the risks of injury.

1.3 RESEARCH QUESTION

What is the influence of increasing inbound mass on the peak dynamic impact response of the Hybrid III head form and brain tissue deformation?

1.4 OBJECTIVES

1. To describe the effects of inbound mass on the dynamic impact response of the Hybrid III head form as measured by peak resultant linear and angular acceleration for centric and non-centric impact conditions.
2. To describe the effects of inbound mass on brain tissue deformation as measured by peak maximum principal strain and peak von Mises stress for centric and non-centric impact conditions.

1.4 EXPERIMENTAL HYPOTHESIS

1. It is hypothesized that an increase in inbound mass will result in a linear relationship for the dynamic impact response and brain tissue deformation characteristics for a centric impact condition.
2. It is hypothesized that an increase in inbound mass will result in a linear relationship for the dynamic impact response and brain tissue deformation characteristics for a centric non-centric impact condition.

1.5 NULL HYPOTHESES

1. Changes in **inbound mass** will have no effect on **peak linear acceleration** for the **centric** impact condition**.**
2. Changes in **inbound mass** will have no effect on **peak angular acceleration** for the **centric** impact condition**.**

3. Changes in **inbound mass** will have no effect on **peak von Mises stress** at the for the **centric** impact condition**.**
4. Changes in **inbound mass** will have no effect on **peak maximum principal strain** for the **centric** impact condition**.**
5. Changes in **inbound mass** will have no effect on **peak linear acceleration** for the **non-centric** impact condition**.**
6. Changes in **inbound mass** will have no effect on **peak angular acceleration** for the **non-centric** impact condition**.**
7. Changes in **inbound mass** will have no effect on **peak von Mises stress** at the for the **non-centric** impact condition**.**
8. Changes in **inbound mass** will have no effect on **peak maximum principal strain** for the **non-centric** impact condition**.**

1.6 SIGNIFICANCE

This thesis is significant in examining the influence of inbound mass on the dynamic impact response and brain response in terms of tissue deformation. It has been suggested that the resulting response curve created from impact is more representative of actual brain injury, as presented as tissue response, than the experienced peak resultant accelerations (Post, Hoshizaki & Gilchrist, 2010). Therefore peak resultant linear and/or angular accelerations may not capture and/or fully represent the complete dynamic response of the head upon impact, and the response occurring at the brain tissue level. This information is important for examining the observed dynamic response, peak resultant linear and angular acceleration of the head, upon and following impact, and the corresponding brain tissue response. This contribution may be used as a guide in managing and predicting the risks of head injury.

Essentially, an injury occurs when the head is subjected to a rapid onset of high forces occurring over a short duration (Barth, 2001). The severity of resulting injury is directly related to the magnitude of the impacting force (Newman et al., 2006). There has been a growing trend in professional sports toward increasing in size of players as a way to improve performance (Neyer, 2001; Montgomery, 2006). This trend has been observed in sports such as football and hockey in which hitting and checking is inherent in the game, and therefore bigger and heavier players can cause serious injuries due to higher body mass/force of impact. Today hockey players are much larger, stronger and faster than they were 70-80 years ago. Athletes playing from 1983-2003 weighed on average 37.5 lbs more and were approximately 10 cm taller than players in 1920s and 30s (Montgomery, 2006). Considering the mass of athletes today striking the head of another player, the force produced by that player will have a direct influence on the resulting acceleration of the head. Therefore this quality of an impact is important to consider when investigating the mechanisms of mTBI.

1.7 LIMITATIONS

1. A 50^{th} percentile adult male head form (Hybrid III) was used in this thesis. The Hybrid III head form, although widely accepted and used as a representation of the human head, is not biofidelic and therefore will not imitate the exact dynamic properties of a human head.
2. The head form is attached to a low resistance sliding table to allow movement of the head after an impact. This effect on the impact mechanics of this table has not yet been well defined.
3. Peak magnitude of the resultant accelerations do not consider direction, which are reflected in the entire dynamic response.

4. The maximal principle strain represents the highest strain value amongst the three axes. Therefore, this is not a global representation of the strain experienced by the brain. Moreover, it is unknown which axis, *x*, *y*, or *z*, experienced the highest strain.
5. The centric impact site chosen for this study (Side Center of Gravity) impacts the head form through the center of gravity of the head, and not through the center of gravity of the head and neck form combination.
6. The University College Dublin Brain Trauma Model (UCDBTM) is the finite element brain model used for this study. The development of this model was based on adult male CT scans of cadavers, however may not be representative of a 50^{th} percentile adult male.

1.8 DELIMITATIONS

1. Impact masses were chosen based on the mass of the metal pendulum system alone without the added metal weight plates. This system weights 4.3 kg, therefore the range of masses investigated in this study were 4.3 – 14.3 kg.
2. The UCDBTM is a partially validated model and therefore the brain stem was not evaluated for this study.
3. The response of the brain model is dependent on the material properties that each respective part of the head/brain complex have been assigned, however variation in the literature suggests that definitive material properties have not yet been established.

CHAPTER 2. LITERATURE REVIEW

Head injuries can be the result of a number of different situations including falls, accidents, and professional or recreational sports. Kleiven (2002, p.1) defines neurotrauma as being "the physical damage that results when the human skull and brain are suddenly or briefly subjected to intolerable levels of energy that is usually transmitted mechanically". Research on the mechanisms by which head injury occurs has dramatically improved our understanding in recent years. Knowledge regarding how the head responds to impacts, and the subsequent brain tissue response, offers important information for managing and reducing risks for head injury. Ultimately, this provides a direction for helmet design and safety standards.

2.1 CLASSIFICATION OF HEAD TRAUMA

Human head injuries have been divided into two main classification types: focal injury, which effect localized regions, and diffuse injury, which occur in a more widespread area (Kleiven, 2002; Bailes & Cantu, 2001). Focal injuries are often the result from direct blows causing tearing and localized injuries. Injuries that have visible local damage such as hematomas and cortical or subcortical brain contusions are considered focal injury (Bailes & Cantu, 2001; McIntosh et al., 1996). Diffuse injuries cannot be seen by the naked eye because these injuries affect neural tissues deep to the skull and include diffuse axonal injury (DAI), and concussions (Kleiven, 2002; Bailes & Cantu, 2001). The severity of diffuse injury varies such as occurring over a continuum of mild to more severe cases of both concussion and DAI and is characterized as shearing of the white matter fiber tracts (Strich, 1961; Adams, Graham, Murray, & Scott, 1982; Gennarelli et al., 1982) manage

Contrary to the success at managing focal type injury, concussions are currently of concern in recreational and professional sports (Delaney et al., 2002; Flik et al., 2005; Casson et al., 2010). Unfortunately, the definition of concussion and severity grading of concussion injuries lack collective agreement due to the diverse affects that injured individuals experience (Leclerc, et al., 2001). In severe cases, post-concussion syndrome is experienced, defined by the presence of at least three typical concussion symptoms up to at least three months post injury (ICD-10, WHO 1989). Most individuals experience post-concussion symptoms, although recovery time from injury widely varies from one person to the next. Most commonly these symptoms resolve within one week to six months (Iverson et al., 2010), however for few people post-concussion symptoms may last for several months (Roe, Sveen, Alvsaker & Bautz-Holter, 2009; Sigurdardottir, Andelic, Roe, Jerstad & Schanke, 2009) having potentially gross effects on daily living, known as post-concussive disorder (Ryan & Warden, 2003; Wood, 2004).

2.2 MECHANISM OF HEAD INJURY (DYNAMIC RESPONSE MEASURES)

Injury results when a tissue exceeds its level of tolerance to a specified load, whether it be acceleration, force, energy or power (Horgan, 2005). In attempts to prevent, or decrease the risks of injury, head injury tolerance criteria have been estimated by relating kinematic data with observed injury outcomes. Through the understanding of the mechanism of head injury, tolerance criteria can provide thresholds or estimated limits identifying the probability of

sustaining and/or preventing head and brain injuries. However, tolerance criteria and helmet safety standards lack complexity in terms of describing performance characteristics of varying impact parameters and are therefore limited in their ability to predict injury risk. The Gadd Severity Index (GSI) and Head Injury Criterion (HIC) is only representative of a single

axis resultant acceleration curve from impacts of one direction and at one location (Gadd, 1966). These two indices were created based on frontal head impacts only using human cadaver and mongrel dogs. A slight improvement is the Head Impact Power index (HIP), although remains location specific, has adopted impact direction sensitivity (Newman, 2000). Current injury threshold measures vary in terms of which impact characteristics are considered in the prediction although are often limited to one biomechanical attribute. Unfortunately for the most part, the existing injury tolerance criteria do not consider the mass of the impact in their formulas. It has been determined that a weighted combination of various biomechanical measures, such as linear acceleration, angular acceleration, impact location, and Head Injury Criteria (HIC) are important to consider when clinically diagnosing concussions and measuring severity, as opposed to any singular impact characteristic (Greenwald et al., 2008). Commonly, helmet safety standards base safety criteria exclusively on linear acceleration as indicators of injury using primarily centric testing protocols (Goldsmith & Plunkett, 2004). However both linear and angular accelerations are important criteria to consider, although one may play a more important role in predicting the different types of head injury. High peak linear accelerations have shown to predict the risk of TBI including, subdural haematomas and skull fracture (Holbourn, 1943; Ommaya & Hirsch, 1971; King et al., 2003), whereas rotational acceleration has been demonstrated to be more closely associated with mTBI, or concussion type injuries **(**Holbourn, 1943; Gennarelli et al., 1982**).** Tolerance indices, and head acceleration have been associated with the type and severity of head injuries, therefore making these measures important to consider when determining the injury risks and prevention.

2.2.1 GADD SEVERITY INDEX / HEAD INJURY CRITERION

In early 1960's the Wayne State Tolerance Curve (WSTC) was the basis to set the foundation that many current accepted indices of head injury are based upon. This curve plotted head linear acceleration against impact durations. It was created from impacts to embalmed anaesthetized primates and canines cadavers, by equating pressure outcomes with linear skull fracture and sub-fracture concussive impacts resulting from high-energy frontal drops onto rigid flat surfaces (Gurdjian, Roberts & Thomas, 1966). The WSTC shows the relationship between the head impacts, in terms of linear acceleration and impact duration, and risks of developing injury, namely fractures of the skull (Gurdjian, Webster & Lissner, 1958). The WSTC indicated that as the duration of an impact increased, the tolerable intensity decreased. This meant that the acceleration or force created by an impact was not the only important criterion for assessing risks to injury or injury thresholds. A limitation of the WSTC is that it did not account for the size and shape of the impact, therefore an extension of this acceleration-time tolerance curve became the Gadd Severity Index (GSI) in 1966 and is used to predict the risks of injury to the brain within a closed environment, comparable to a helmeted head (Gadd, 1966). Dissimilar from the WSTC, the GSI proposed a log-log scale to plot the curve as a straight line with a power-weighing factor, from which a numerical value could be used to define injury threshold. This threshold, known as the GSI is calculated as follows;

$$GSI = \int_{t_0}^{t} \bar{a}^{2.5} dt$$

Where:
a = acceleration (g) at the center of mass
n (2.5) = power weighting factor used for head impacts
t = time (seconds)

where *a* is the peak linear acceleration vector of the head form's center of gravity in standard gravitational units (*g*) to the power-weighting factor of 2.5 and integrating it over impact time *t* in seconds (s). The GSI is often used for the assessment of new helmets and helmet technology because of its ability to predict risks within a closed environment. Helmets surpassing a calculated severity index (SI) of 1000 are considered unsafe and life threatening, carrying high risks of head injury (Gadd, 1966). The weighing factor of 2.5 is based on the slope of the WSTC between 4 and 50ms, and was originally intended to predict frontal impact injuries, however is currently being used for several other impact sites. A refinement of the GSI, in 1972 the National Highway Traffic Safety Administration (NHTSA) proposed the Head Injury Criterion (HIC) that uses head forms for safety standards and head protection establishments. The HIC is based on the resultant translational or linear accelerations multiplied by the change in time in order to account for long duration impacts of low acceleration (Versace, 1971). The formula for the HIC is;

$$HIC = (t - t_0)\left[\left(\frac{1}{t - t_0}\right)\int_{t_0}^{t} \vec{a}\,(t)\,dt\right]^{2.5}$$

Similar to GSI '*a*' and '*t*' are used in the HIC formula, however '*t* to t_0' are also measured as the initial and final time of the interval duration in which HIC attains the maximum value. However the maximum time duration of HIC is limited to a specific time, often 15ms. One of the limitations of the HIC is that it does not provide injury prediction thresholds for impacts of varying direction. In addition, an inherent concern with these criterion is their inability to account for angular accelerations, the complex brain skull interaction, and the deformation of neural tissue. Regardless of these drawbacks, the HIC is the most widely

used head injury criterion today. A notable aspect is the similarity between the equation for GSI and the equation

for a change in momentum, or an impulse and is defined as the integral of force with respect to time.

$$Impulse = \int F dt$$

Where,
F = the instantaneous force;

The Gadd Severity Index is determined by the instantaneous acceleration, as acceleration due to gravity rather than force. As force is proportional to mass and acceleration, the GSI has failed to account for the effect of mass on predicting the risks to injury.

2.2.2 GENERALIZED HEAD ACCELERATION MODEL FOR BRAIN INJURY THRESHOLD (GAMBIT)

In 1986 Newman acknowledged that rotational acceleration may have considerably more damaging effects than pure translation, and proposed that both linear and angular acceleration in combination can cause head injury. The original Generalized Head Acceleration Model for Brain Injury Threshold (GAMBIT) was developed that considers both linear and angular acceleration, and direct and indirect impacts in its head injury criterion. It was defined as;

$$G(t) = \left[\left(\frac{\vec{a}(t)}{\vec{a}_c} \right)^m + \left(\frac{\vec{\alpha}(t)}{\vec{\alpha}_c} \right)^n \right]^{\frac{1}{2}}$$

Where,
G(t) = the instantaneous measure with a threshold of 1;
a(t) = the instantaneous linear acceleration at time t;
α(t) = the instantaneous angular acceleration at time t;
a_c = the critical value for linear acceleration;
α_c = the critical value angular acceleration;

m, *n*, and *s* are empirical constants set to match the data set: linearly weighted model = 1: elliptical model = 2.

The GAMBIT model was developed from automotive accident reconstructions based on their respective hospital records. This original GAMBIT model has undergone various revisions, however currently uses maximal linear and angular acceleration values to calculate injury severity thresholds. Unfortunately the GAMBIT lacks validation and is therefore not often used or required for any regulations.

2.2.3 HEAD IMPACT POWER

Most recently Newman et al. (2000) recognized the drawback to both GSI and HIC and proposed the Head Impact Power (HIP). The HIP criterion integrates direction sensitivity based on reconstructed American football head collisions. HIP is defined by the following equation;

$$HIP = \left(m\vec{a}_x \int \vec{a}_x dt\right) + \left(m\vec{a}_y \int \vec{a}_y dt\right) + \left(m\vec{a}_z \int \vec{a}_z dt\right) + \left(I\vec{\alpha}_x \int \vec{\alpha}_x dt\right) + \left(I\vec{\alpha}_y \int \vec{\alpha}_y dt\right) + \left(I\vec{\alpha}_z \int \vec{\alpha}_z dt\right)$$

where mass and angular momentum are integrated into the formula. Although the HIP does integrate directional components, because the final criterion established is a single value, it does not provide an explanation for the cause of any change, such as location of impact.

2.2.4 LINEAR ACCELERATION

When the head is impacted, the experienced acceleration is the result of the forces generated by the collision (Newman, 1993). There has been some discrepancy between findings relating linear acceleration as a mechanism of head injury. However this type of acceleration has been associated with a multitude of head injury types, and is believed to be linked with focal type injuries, or traumatic events resulting from pressure gradients throughout the brain

and/or skull deformation (Holbourn, 1943; Gennarelli, Thibault & Ommaya, 1972; King et al., 2003).

Many researchers in as early as in the 19th century discovered intracranial pressure changes at the time of impact although its relevance to injury varied amongst these experiments (Gurdjian, 1975). However, a commonality was that blunt impacts to the head resulted in intracranial pressure changes as well as deformations of the skull, and that the experienced pressure changes were found to be more related to the acceleration and deceleration caused by impact than was skull deformation (Gurdjian, 1975). Therefore linear acceleration was determined as a measure of injury as it represented the internal pressure changes resulting from impact based on this relationship. In addition, this measurement was used because at this point in time, linear acceleration was a variable that was actually measurable, despite the hypothesized influence of rotational acceleration (Holbourn, 1943).

The mechanisms for traumatic injury were of interest to Gurdjian, and colleagues in 1963. Their study involved work with mongrel dogs, and found that angular acceleration alone could not cause enough damage to the brain to result in injury. Therefore the conclusions drawn indicated that linear accelerations were important to consider for injury mechanisms. Ono and researchers (1980) also found from their study on traumatic brain injury in monkeys that linear acceleration had a high correlation with the incidence of concussion. Furthermore, it was concluded and no relationship was observed between the incidence of mTBI and angular accelerations.

Currently, helmet safety standards use peak linear acceleration as validation criteria. A limitation to using peak linear acceleration as a measure of injury is that is neglects to provide information about the motion of the head as it only represents one moment in time (the peak) and does not describe the shape of the impact loading curve, and therefore

possibly not exemplifying brain injury (Post et al., 2010). However this measurement is still commonly used to describe injury and injury thresholds for helmet standards and therefore must be considered.

2.2.5 ANGULAR/ROTATIONAL ACCELERATION

Protective headgear is designed to decrease injury risks by lessening the acceleration experienced by the head though energy attenuation, however typically decreases the risk of TBI by attenuating linear acceleration, and are not designed to attenuate rotational acceleration. Contrary to the assumption that linear and angular accelerations are highly correlated, research has reported that helmets that have the ability to decrease linear acceleration from impacts, may not manage angular acceleration as effectively (Hoshizaki & Brien, 2004; King et al., 2003; Rousseau et al., 2009). Moreover Walsh and colleagues (2011) found only moderate correlation (r2=0.401) between peak linear and peak angular acceleration when helmets weren't involved, therefore indicating that a change in one form of acceleration may not cause the same change in the other. Impacts to the head however, will result to some degree of both linear and angular acceleration (Rousseau et al., 2009). Due to the anatomy of the human head and neck, the impacting force can be expressed as an applied torque where the angular, or rotational acceleration is a result of its magnitude (Newman, 1993). This can be seen in the following equation;

$$T = I\alpha$$

Where:
T = applied torque
I = moment of inertia ($kg.m^2$)
α = angular acceleration (rad/s^2)

A number of studies report a relationship between rotational acceleration and both focal and diffuse type brain injury, and declare that linear acceleration has little effect on injury

mechanisms (Holbourn, 1943; Unterharnscheidt and Higgins, 1969; Gennarelli, et al., 1972; Gennarelli, Abel, Adams & Graham, 1979). A common conception is that the brain rotation that happens inside the skull causes shear stresses and strains, and it is these mechanisms that result in injury (Holbourn, 1943; Hodgson & Thomas, 1979).

The notion that mTBI is caused mainly by rotational acceleration was first introduced by Holbourn (1943). Holbourn suggested that shear strains within the brain are the main cause of injury, and because linear acceleration forces produce compressional strains, they don't have an injurious effect. He demonstrated this theory by comparing the skull brain interaction with an image of giving a sudden rotation to a flask full of water. The water will tend to stay in place as the glass flask will rotate around it. However, the water attached to the inner surface of the flask will rotate with the flask separating from the other water particles, thus producing large shear strains. Concluding that rotation has a far greater influence than translation and only shear stresses and strains were responsible for injury due to the nearly incompressibility of neural tissue (Holbourn, 1943).

Based on Holbourn's theories, Unterharnscheidt and Higgins (1969) created brain injury in squirrel monkeys including subdural haematoma, tearing of bridging veins, and lesions. These injuries were reported to be the result from applying a controlled angular acceleration.

Another study performed by Gennarelli and colleagues (1972) using squirrel monkeys revealed an increased frequency and severity of cerebral concussion in monkeys who experienced rotation of the head over purely translation. It was noted that although pure translation created higher magnitudes of peak g levels (665-1230g), over the rotation group g levels (348-1025g), all monkeys who experienced rotation were concussed, contrary to the pure translation group (Gennarelli et al., 1972).

Hodgson and Thomas (1979) experimented with hemi-section models of monkey brains. They exposed these models to three different types of impacts; pure translation, pure rotation, and combined translation and rotation. Peak linear and angular accelerations were measured in addition to shear strain production in different parts within the brain, and relative brain displacement. Angular acceleration was reported to be the primary source of shear strain and brain displacement, where the highest values occurred within the brainstem (Hodgson & Thomas, 1979).

A multitude of types of head injuries were produced among 53 adult subhuman primates as a result of a single sagittal plane angular acceleration (Gennarelli et al., 1979; Adams, Graham, & Gennarelli, 1981). Injuries that were seen among these primates included fracture of the skull, subdural haematoma, contusions, and discrete intracerebral haematoma. Despite the research relating angular acceleration to injury, existing helmet standards do not consider this variable when testing helmet safety. However, the University of Ottawa Testing Protocol (uOTP) was recently developed as the first protocol to consider both centric and non-centric impacts. Nine impact conditions (locations and angles) were identified by Walsh and colleagues (2011) as producing either a peak linear or peak angular acceleration value beyond an 80% probability of sustaining mTBI according to estimated injury thresholds published by Zhang, Yang, and King (2004). Of the nine conditions identified, five were selected as the testing protocol. To avoid an order effect, one impact from each of the five sites at the angle that posed the highest risk was chosen (Walsh et al., 2011). The objective of this protocol is to consider both linear and angular accelerations when testing helmet performance so as to decrease risks for head injury.

2.3 INFLUENCE OF IMPACT CONDITION ON THE DYNAMIC RESPONSE

Head injury is the result of the head acceleration experienced during impact. Each direct impact to the head creates a three-dimensional dynamic response measured as linear (translational) and angular (rotational) accelerations upon the *x*, *y*, and *z*-axis, which defines the sequence of motion. The resulting dynamic response curves vary as the impact characteristics change, such as impact site, mass, velocity, angle of impact, and compliance of impactor, consequently resulting in unique dynamic and different head and brain injuries (Gennarelli et al., 1982; 1987; Zhang et al., 2001; Kleiven, 2003, Pellman et al., 2003). How variation in impact conditions effect the dynamic response can aid in the understanding of managing and reducing risks to injury. Impact parameters such as impact site, velocity and angle have been shown to influence the resulting dynamic response of the head, however how an increasing inbound mass effects the head response has not been fully described. According to the literature, frontal impacts do not provide a valid representation of head impacts of varying directions (Gennarelli, 1979; Zhang et al., 2001; Kleiven, 2003). Moreover, by testing the dynamic response of frontal impacts to determine risks for injury, underestimation of the severity of injury may be of concern. Often lateral impacts have presented higher risks for injury compared with other impact locations under the same impacting events. (Gennarelli et al., 1979; Zhang et al., 2001; Zwahlen, Labler, Trentz, Gratz & Bachmann, 2007). In order to identify head injury thresholds to decrease the risk of head injury, it is imperative that the variation in dynamic impact response account for different impact conditions, in this case, impact location.

The direction or vector of the applied force, or impact site in relation to the center of gravity of the head will have an effect on the dynamic impact response outcome (Barth et al., 2001). Impacts to varying locations and at different angles have been shown to produce different

magnitudes of peak resultant linear and angular accelerations, where one was not indicative of the other (Walsh et al., 2011). Impacts off the center of gravity create higher angular accelerations (Nusholtz, Melvin, & Alem, 1979; Walsh et al., 2011). Nusholtz and coworkers demonstrated this by producing different magnitudes and directions of rotation by experimenting with three impact sites on primates.

2.3.1 IMPACT SITE

The site on the head where to the impact happens has also been shown to have an influence on the resulting brain response, and therefore resulting head injury (Gurdjian, Lissner, Latimer, Haddad & Webster, 1953; Gennarelli et al., 1982; 1987; Hodgson, Thomas & Khalil, 1983; Zhang et al., 2001).

Laboratory tests performed on dogs revealed that the site of the blow had a marked effect on the concussive response of the animal (Gurdjian et al., 1953). Blows to the occipital protuberance showed more serious concussive outcomes, whereas blows to the parietal area and the sagittal crest were found to have lower potential consequences. It should be noted however, that this research involves dogs, and due to head geometry differences, these findings were not consistent with experiments using primates and human head data (Gennarelli, et al., 1982; 1987; Hodgson et al., 1983; Zhang et al., 2001; 2004; Zwahlen et al., 2007).

Gennarelli and colleagues (1982; 1987) demonstrated experiments using primates that led to conclusions that lateral direction rotational accelerations compared to anterior and posterior rotational accelerations were a more important contributor to concussion. These researchers found that non-centroidal coronal rotation resulted in longer lasting comas over acceleration in both the sagittal and horizontal directions (Gennarelli, et al., 1982). Animals subjected to

lateral impacts displayed DAI in the corpus callosum and brain stem to a comparable degree of severe human brain injury (Gennarelli, et al., 1982; 1987).

Hodgson et al. (1983) also studied the effects of impact site to determine tolerance to concussion. Anesthetized monkeys were exposed to front, side, rear and top impacts while wearing protective caps. Side impacts were found to produce the highest magnitudes of both linear and angular accelerations, accompanied by the longest periods of unconsciousness, revealing a decreased tolerance to concussion (Hodgson et al., 1983).

Researchers Zhang, Yang and King (2001; 2004) identified differences in skull deformations and relative brain dynamic responses between frontal and lateral impacts. Their research employed finite element analyses to model location specific head impacts. Higher positive pressure and shear were found from lateral impacts, especially at the core region, known as the middle of the brain. (Zhang et al., 2001; 2004).

In 2007, researchers assessed computed tomography scans of patients with severe closed head injuries and concluded that impact site may be an indicator of diffuse axonal injury. Namely lateral impacts being responsible for a much higher risk than frontal and oblique impacts (Zwahlen et al., 2007)

2.3.2 ANGLE OF IMPACT

Limited research on the effects of impact angle on the resulting dynamic response of the head has been performed however, is an important variable to consider when examining the rotation of the head resulting from impact. When a force is applied to a rigid body in one axis, it created rotation about the other two axes proportional to the perpendicular distance away from those axes.

A recent study compared resulting peak linear and peak angular accelerations of impacts of varying angles to three different impact sites (Walsh & Hoshizaki, 2010). Impacts to a 50th

percentile head-and neck form were performed for seven impact angles, through the center of gravity, and at 5, 10 and 15 degree increments in both positive and negative directions. Peak linear acceleration showed a trade-off effect for x and y vector components with changing impact angle, meaning as one increased, the other would decrease (Walsh & Hoshizaki, 2010). However the z axis component remained inconsequential in peak linear acceleration magnitude with changing impact angle. The vector components varied significantly, although resultant acceleration remained uniform for two of three impact sites (Walsh & Hoshizaki, 2010). Peak angular acceleration component vectors also varied with impact angle, however did not show an obvious pattern as with linear acceleration. Varying the impact angle at the side impact site produced a dramatic curve in rotation about the *z* axis as a result from *x* and *y* components of linear. Overall, the results from this experiment indicated that inbound vector angle variation may result in a different dynamic response of the headform as seen through peak linear and peak angular acceleration, particularly in the individual component vectors (Walsh & Hoshizaki, 2010).

2.3.3 IMPACT MASS

To date there has been little research done on the effects of inbound mass on the resulting dynamic response of the head or risks to injury. Research has focused mainly on the influence of variable head mass on the impact response and their implications to helmet performance (Gimbel & Hoshizaki, 2008; Kleiven & von Holst, 2002).

Hodgson and coworkers (1967) however used variable impact mass and velocity to study the tolerance of facial bones to fracture. In determining differences between various areas of the facial bones, solid metal cylinders were used for impacts with mass ranging from 0.9 kg to 7.9 kg (Hodgson, 1967). The impactor mass in this experiment was used to vary the force of

the blow. The primary conclusion of this research was that as the force of the impact increased, the time to fracture decreased (Hodgson, 1967).

Kleiven and von Holst (2002) examined the effects of different head size on the intracranial response of the human head. This study used finite element modeling to perform impact simulations representing various head sizes and mesh densities. The results from this experiment showed that maximal shear stress and maximal von Mises stress, along with intracranial pressures within the brain increase with increasing head size when undergoing the same acceleration pulse (same HIC value) (Kleiven & von Holst, 2002). Contrary to these findings, increasing head size during frontal impacts to a padded surface produced lower HIC values than the overall smaller head sizes. Adding padding to the impact increases the overall duration of an impact (Nahum et al., 1977; Kleiven & von Holst, 2002). The HIC criterion have an inverse relationship with time, therefore for a longer duration impact, a higher HIC value is expected (Versace, 1971). As the size of the head decreases, less energy is absorbed through material compression and therefore results in shorter impact duration and consequently a higher HIC value (Post, Gimbel & Hoshizaki, 2011).

Gimbel & Hoshizaki in 2008 granted attention toward helmet safety standards and design for children. Their research examined the differences in helmet performance, quantified as peak linear acceleration, based on variable head form mass and inbound velocity (Gimbel & Hoshizaki, 2008). They concluded that these variables played a significant role in the performance of the material characteristics in helmet liners and therefore should be considered in helmet testing protocols when designed for specific age groups (Gimbel & Hoshizaki, 2008).

Research conducted on the effects of ball heading in soccer, have examined the influence of ball mass on the dynamic response of the head. Shewchenko and colleagues (2005)

investigated whether ball construction characteristics have the ability to reduce the head and neck impact response resulting from heading. They determined that a lighter ball mass provides a benefit for all of the response measures that were examined. A linear relation was observed between peak resultant linear acceleration and ball mass, with a similar relationship for peak angular acceleration. A decrease in ball mass of 21-35% resulted in reductions of up to 23% in the measured head/neck responses (Shewchenko, Withnall, Keown, Gittens & Dvorak, 2005). However, these authors noted that soccer balls of different manufacturing were used in this study and therefore the variation in mass may not be the only influential parameter tested. Similarly, Harrell and co-workers studied the influence of contact mass during purposeful and accidental heading of a soccer ball. It was found that when the heading of the soccer ball was purposeful, and performed with proper execution, the impact response produced was not adequate to result in injury, based on an HIC of 1000 (Harrell et al., 2004).

In general during scenarios where the players are anticipating contact, the effects of the impacting mass may be lessened because players have the opportunity to prepare themselves and this typically results in a more linear acceleration (Barth et. al, 2001). However in cases where the collision is unexpected, the impacting force creates torque, seen as head rotation, which have more severe outcomes (Barth et al., 2001). Pellman and colleagues (2003) demonstrated this effect of impacting mass through NFL impact reconstructions based from video analysis. In a player-to- player impact, typically the struck player was unaware of the striking player, yielding a higher effective mass for the striking player, because initially only the struck player's head is involved in the impact. This then resulted in rapid changes of head velocity (Pellman et al., 2003). Research on boxing techniques, has also demonstrated the influence of effective mass on the severity of the punch. Study by Smith and Hamill (1986)

compared fist velocity and punching bag momentum between boxing punches of both different skill level boxers and glove types. Their conclusions revealed that there were no differences observed in fist velocities for either skill level or glove type. However the greatest bag momentum was generated by the highest skilled punchers, therefore demonstrating the skilled boxer's ability to generate a greater effective mass during the strike. They estimated the punch mass to be 4.1 kg, which is greater than the mass of the hand. In addition, Walilko, Viano and Bir (2007) examined the punch forces generated by Olympic boxers from five different weight classes. These researchers found that the higher weight class boxer's demonstrated more ability to generate a high punch force, where punch force was the strongest predictor of severity outcomes (HIC, rotational acceleration etc.). The boxer's hand velocity had no significant correlation with weight class, peak punch force, or the severity of the punch, therefore it was concluded that the effective mass of the punch was more important in determining the severity of the impact.

2.4 BRAIN TISSUE DEFORMATION

Although experiments using human cadavers can be appropriate for research that involves gross material properties and/or the kinematic response of the head, it is unable to offer information regarding muscle activation, functional changes and cellular/vascular response. In addition, human head cadavers tend to be of an older age and therefore may not represent the general public (Viano et al., 1989). Technological advancement in finite element modeling (FEM) has allowed researchers to view injury risk from a brain tissue standpoint (Zhang, et al., 2003; 2004; Horgan & Gilchrist, 2003; 2004; Willinger & Baumgarthner, 2003; Kleiven, 2007). The use of mathematical models offers some advantages to these limitations as they attempt to represent the actual human system. Experiments using FEM have a high degree of repeatability through very detailed and controlled tests. These tests

have the capability to represent the material properties of brain tissue and demonstrate their respective sensitivity to varying mechanical inputs (Horgan, 2005). Research has indicated that brain deformation variables show good prediction of concussion type injuries. Through the use of finite element modeling, the researcher has additional information into the effect of the impact on the deformation of brain tissue and potential injury. (Forero Rueda et al., 2010). Both linear and angular acceleration equations assume the head to be a rigid body. Finite element models have been developed to account for the material characteristics of the brain allowing for the interpretation of linear and angular acceleration loading curves and how they influence the response of neural tissue.

2.4.1 HUMAN HEAD ANATOMY

The human brain or the encephalon is divided into three main parts known as the forebrain, the midbrain and the hindbrain (Carpenter, 1991; Gardner, 1975). The forebrain is divided into the telencephalon, consisting of the paired cerebral hemispheres, and the diencephalon, which is the most rostral portion of the brain stem. The midbrain is known as the mesencephalon, and the metencephalon (pons), the myelencephalon (medulla oblongata), and the cerebellum make up the hindbrain (Carpenter, 1991; Gardner, 1975). The brainstem consists of the midbrain, the diencephalon, the pons, and the medulla oblongata, which collectively form the central stalk connecting the cerebral hemispheres and the spinal cord (Carpenter, 1991; Gardner, 1975).

2.4.2 FINITE ELEMENT MODELLING

Three-dimensional finite analysis is used to describe the response of human brain tissue during and following impact. Due to the complexity of anatomical constituents and material component, new model development has focused on improving the accuracy of finite

analysis in terms of the methods, impact locations, and anatomical structures, to better predict risks for injury.

One of the first three-dimensional head model was developed by Ward and Thompson (1975), which was validated against direct frontal impacts to cadaver heads. Human head anatomy was described as linear elastic and included the brain, dura folds, ventricles and brain stem. The skull and CSF in this model was assumed as rigid, and did not include the falx and tentorium. This model was validated against experiments by Nahum et al. (1977) on cadavers, although only for frontal impacts.

In the early nineties, Ruan, Khalil and King (1993) and Zhou (1995) developed version I of the Wayne State University brain injury model (WSUBIM) which was also validated against one set of intracranial pressure data from Nahum et al.'s (1977) cadaveric experiments. The simulations revealed the importance of being able to distinguish between the grey and white matter with in the brain, as well as the inclusion of ventricles. This model was used to determine sensitivity of the brain to impacts from varying directions. Results revealed that the head was more sensitive to lateral impacts compared to impacts to the front of the head. Sagittal plane impacts created higher intracranial pressures, skull deformation, and shear strains, especially within the core region of the brain. The researchers also hypothesized that strain levels within the genu could be used to predict diffuse axonal injuries (DAI) due to its anatomical components and distinguishing material properties between white and grey matter.

A later version of the WSUBIM, version II, was created by Al-Bsharat et al. (1999) with an added characteristic of a sliding skull/brain interface. This model was the first to represent the relative motion between the skull and brain with a sliding interaction, and was validated against the majority of the pressure data by Nahum et al. (1977).

In 2001 Zhang and associates recognized the limitation of 3D finite element head models to date, indicating that previous head models were limited to frontal intracranial pressure response, and therefore produced WSUBIM version III that consisted of the highest density mesh and detailed facial structure to date. This was a highly complex very finely meshed model consisting of over 281, 800 nodes, and 314, 500 elements was able to improve the detail and accuracy of each anatomical feature including; the scalp, skull, diploe, dura, falx, cerebri, tentorium, pia, sagittal sinus, transverse sinus, CSF, cerebrum with grey and white matter, cerebellum, brainstem, lateral ventricles, third ventricles, and bridging veins (Zhang et al., 2001b). The CSF was modeled with solid elements with material properties of bulk modulus and a very low shear modulus. The sliding characteristic between the dura and arachnoid membrane introduced by this model was suggested to be a more realistic representation of human head kinematics (Pudenz & Shelden, 1946; Meaney, 1991). A noted limitation of this model, and 3D models of the past, was their inability to predict representative brain responses, due to the lack of documentation on real-world head injury simulation and validation.

Kleiven and Hardy (2002) examined how assigning different material properties to the brain tissue and/or brain-skull interface can impact the results obtained from injury simulations. These researchers constructed a 3D model capable of geometric adjustments to fit specific specimens and/or populations. The head model consisted of; the scalp, skull, brain, meninges, CSF, and parasagittal bridging veins. Also modeled was a neck consisting of an extension of the brainstem to the spinal cord, dura mater, pia mater, vertebrae, and muscles. Simulations were performed under three different skull-brain interfaces, and three differing brain tissue material properties. Results for each simulated condition was compared against cadaver experiments by Nahum, Smith and Ward (1977) and Trosseile, Tarriere, Lavaste,

Guillon and Domont (1992) for intracranial pressure changes and Hardy, Foster, Mason, Yang and King (2001) for relative motion between the skull-brain. Some major findings were; the type of allocated brain-skull interface was more influential to the pressure response than the brain tissue constituents; the skull-brain interface chosen had little effect on local brain motion for impacts of low severity; lateral impacts result in less relative brain-skull motion than frontal or occipital blows; and local brain motion response was sensitive to the shear properties of brain tissue, with averaged published values showing the highest correlation with experiments.

In 2003 Horgan and Gilchrist constructed a 3D finite element model for the purposes of simulating head impacts resulting from pedestrian accidents. A variety of model types were created with mesh of varying densities and different element formulations that were compared and validated against experimental cadaver data of Nahum et al. (1977). The geometry of the model was created from Computed Tomography (CT) scans of human male cadaver models and includes; the scalp, 3-layered skull, dura, CSF, pia, falx, tentorium, cerebral hemispheres, cerebellum, and brainstem. The researchers examined the effects of bulk and shear modulus of the brain and CSF by way of a parametric study. Their results revealed that intracranial pressure and von Mises response was largely effected by the short-term shear modulus of brain tissue, and the bulk modulus had the greatest effect on the contre-coup pressure when CSF was modeled using a coupled node definition. Based on observed intracranial pressure differences, Horgan and Gilchrist (2003) highlight the necessity of careful modeling for the depth and volume of CSF, and thickness of the skull, in order to predict accurate pressure distribution. The weight of this head model was scaled to the dimensions obtained from 37 cadaver skulls from Nahum et al.'s experiment, and is 4.017 kg with the brain weighing 1.422 kg. This model consists of 7,318 solid elements

representing the brain, and 2,874 elements representing the CSF, all composed only of hexahedral elements for the purpose of keeping the number of elements low. In addition, this also improves its capability to model non-linear actions (Horgan & Gilchrist, 2003).

2.4.3 NEURAL TISSUE DEFORMATION METRICS

Based on actual injury reconstruction and finite element modeling, researchers have measured a variety of brain deformation variables and have highlighted the best predictors of brain injury.

Research has demonstrated the relationship between local mechanical deformation and brain injury. Brain deformation variables including strain (Bain & Meaney, 2000; Zhang et al., 2003; Kleiven, 2007), strain rate (Galbraith, Thibault & Matteson, 1993; Zhang et al., 2003) product of strain and strain rate (King et al., 2003; Zhang et al., 2003), maximum principal strain (Kleiven, 2007), Von Mises stress (Willinger et al., 2000; Anderson, Brown, Blumbergs, McLean & Jones, 2003; Willinger & Baumgartner, 2003; Kleiven, 2007), and shear stress (Zhang, Yang & King, 2004), have all been associated with, and deemed useful in, predicting injury risk. Frequent brain deformation metrics used in the analysis of brain injury prediction and risks are maximum principal strain and von Mises stress.

The maximum principal strain is described by tissue elongation relative to its original length. This elongation occurs in the tissue along one of the principal axes (Silva, 2006). This dependent variable is commonly used in finite element modeling of head injury to indicate brain deformation resulting from an impact. A limitation of maximal principal strain measurement is that it only represents the elongation along the principal axis with the largest value. This assumes that the largest value describes the mechanism of injury, which may not be true (Silva, 2006).

The calculation of von Mises stress as a dependent variable for brain deformation is used for complex loading scenarios (Silva, 2006). Basically, this equation establishes the deformation of a structure by considering all the various tensors involved. The result is determined as a uniaxial strain, which can be compared to the literature (Silva, 2006). This purpose of this calculation is that it can take the sum of all the tensors involved and report as one value in units of pressure. This deformation metrics accounts for different directions of strain upon an element and is therefore commonly used among researchers (Silva, 2006).

Stress and strain within the brain occurs as a result to impact of the head and has been demonstrated through accident reconstruction (Zhang, et al., 2003; Horgan & Gilchrist, 2003; 2004; Kleiven, 2007). Finite element analysis has been used to study the role that both linear and angular acceleration play in strain-induced head injuries. Research has indicated that rotational acceleration highly contributes to brain strain and stress (Zhang, Yogandan, Pintar & Gennarelli, 2006a: 2006b; Forero Rueda, et al., 2010), where 80% and 90% of strain within the brain was attributed to rotational acceleration (Zhang et al., 2006a; 2006b) Recent work employing the UCDBTM for analysis of simulated helmeted head impacts found linear acceleration to show low correlations ($r^2 = 0.20 – 0.52$) with peak and average Von Mises stress and maximum principal strain. This investigation reported that linear acceleration is a poor predictor of tissue response, specifically peak and average maximum principal strain and peak and average Von Mises stress, when location of an impact is not considered. However angular head accelerations showed higher correlations with peak and average Von Mises stress ($r^2 = 0.72 – 0.79$) and maximum principal strain ($r^2 = 0.70 – 0.75$) outputs even without impact location differentiation (Forero Rueda, et al., 2010).

2.5 PROPOSED INJURY THRESHOLDS

2.5.1 DYNAMIC RESPONSE THRESHOLDS

A variety of methodologies have been used to estimate injury thresholds for sustaining an mTBI based on the resulting head kinematics of an impact (Table 1). Zhang et al. in 2004 proposed injury threshold values based on a 25 %, 50 % and 80 % probability of sustaining an mTBI for peak resultant translational accelerations, and peak resultant rotational accelerations. Estimated values for translational acceleration were 66, 82, and 106 g and rotational acceleration values of 4600, 5900, 7900 rad/s^2 were correlated with mTBI probability respectively. Although, Willinger and Baumgarthner (2003) found that mTBI injury was probably when angular head accelerations of approximately 3000-4000 rad/s^2 were experienced.

Table 1: Estimated mTBI injury thresholds, based on peak linear and angular accelerations.

Methods	Estimated Thresholds	Researchers
Primate, Cadaver	90 g 1800 rad/s^2	Gurdjian et al. (1966) Ommaya et al. (1967)
Instrumented Helmets	81 g 82-146 g	Duma et al. (2005) Schnebel et al. (2007)
Laboratory Reconstructions	82 g = 50 % 5900 rad/s^2 = 50 % 3000-4000 rad/s^2	Zhang et al. (2004) Willinger & Baumgarthner (2003)

2.5.2 BRAIN TISSUE TOLERANCE THRESHOLDS

Finite element modeling has also been used to establish estimated thresholds (Table 2). These aim to make associations between the mechanisms of the injury and an engineering variable represented by the deformation characteristics of brain tissue. In 2003, real world head injury simulations done by Willinger & Baumgarthner found that von Mises stress values of 18 kPa and 38 kPa were indicative of a 50 % risk of moderate and severe

neurological lesions respectively. Zhang and colleagues (2003) established threshold values for a 25 %, 50 %, and 75 % probability of sustaining a concussion and were estimated for strain, strain rate, and product of strain and strain rate at the midbrain region. Strain levels were 0.25, 0.37, and 0.49, estimates for strain rate were 46, 60, and 80/s, and for product of strain and strain rate, thresholds of 14, 19, and 24/s, were established, respectively. Furthermore, Zhang et al. in 2004 proposed injury thresholds based on a 25 %, 50 % and 80 % probability of sustaining an mTBI for shear stress in the midbrain were estimated as 6.0, 7.8, and 10.0 kPa, respectively. Most recently, Von Mises stress of 8.4 kPa and maximum principal strain of 0.21 or 0.26, depending on location within the brain tissue, were identified with 50% probability of concussion (Kleiven, 2007).

Table 2: Estimated mTBI injury thresholds based on brain tissue deformation.

Brain Location	Deformation Variable	Estimated Thresholds	Researchers
Grey matter Brain stem	Max principal strain Von Mises stress	0.19 7.8 kPa = 50 %	Zhang et al. (2004)
Corpus callosum Grey matter Corpus callosum	Max principal strain Max principal strain Von Mises stress	0.21 = 50 % 0.26 = 50 % 8.4 kPa	Kleiven (2007)
N/A	Von Mises stress	18 kPa (moderate) 38 kPa (severe)	Willinger & Baumgarthner (2003)

CHAPTER 3. METHODOLOGY

The main objective of this study was to determine the effects of impact mass on the dynamic impact response (peak resultant linear and peak resultant angular acceleration) of the unhelmeted Hybrid III head form, and brain tissue response, as represented through finite element modeling (FEM). Alteration of the Hybrid III head form position about the *x, y*, and *z-axes* will allow for discriminate between impact conditions. The Hybrid III head form was impacted at one centric (Side Center Gravity) and one non-centric (Front Boss 45° Positive Azimuth) impact site based on the University of Ottawa Testing Protocol (uOTP) (Walsh et al., 2011). Impacts at each site were performed with various impact masses at 2 kg increments: 4.3 kg; 6.3 kg; 8.3 kg; 10.3 kg; 12.3 kg; 14.3 kg. Each impact condition was performed at a velocity of 4.0 m/s. The dynamic response of the Hybrid III head form was measured using a "3-2-2-2" array of accelerometers mounted orthogonally in the Hybrid III head form (Padgaonkar, Krieger & King, 1975). This dynamic response, specifically the *x*, *y*, and *z* components for both linear and angular acceleration were used as an input for the UCDBTM to determine the deformation response characteristics, von Mises stress and maximum principal strain, within the brain tissue.

3.1 DYNAMIC IMPACT TESTING

3.1.2 PENDULUM SYSTEM

The impacts for this study were performed using a pendulum system. This impacting system was a hollow metal frame weighing 3.36 kg (Fig. 1) and was suspended using 3/32" aviation cable (length 9.25 ft.). The impactor was free to swing using four cables attached to ceiling-mounted metal beam directly above the head form. Circular metal plates weighing 1 kg and 2 kg were fastened into the center of the cylinder to achieve the appropriate mass (Fig. 1). A

hemispherical nylon striker (diameter 12.6 cm, weight 0.92 kg) containing a compliant 25.4 mm modular elastomer programmer (MEP) 60 Shore Type A middle layer pad, was attached to the impacting end of the pendulum cylinder (Fig 1). MEP is a stiff material that offers very little compliance and therefore may have the least amount of influence on the results in terms of energy absorption. Therefore it was chosen as the impact surface for this study so that effects of varying inbound mass were measured via the response of the head, rather than the response of the impacting surface. In addition, this is a common material used in helmet standard testing protocols (CAN/CSA-D113.2-M89, 1996; NOCSAE *001-06m07*, 2007). The hybrid III head and neck form was attached to a low-friction sliding table. The sliding table (12.782 ± 0.001 kg), allows the head form to be adjusted within 6 degrees of freedom, and is mounted on rails to provide a low friction surface. The low friction system allows the head form to slide upon impact. The pendulum system was positioned so that the center of metal steal frame was aligned with the impact site on the head form. The following equations were used to estimate the angle and height at which the pendulum was released to achieve a velocity of 4.0m/s;

$$v = 2g\left[L - Lcos\left(\theta\right)\right]^{\frac{1}{2}}$$

Where,

v = the velocity of the weight at the bottom of the swing;
g = the acceleration due to gravity;
L = the length of the wire;
θ = the angle from the vertical;

$$h = L - Lcos\,(\theta)$$

Where,

h = starting height from bottom of free hanging pendulum;
L = the length of the wire;
θ = the angle from the vertical;

For each impact the pendulum was released by switching off a magnet holding the pendulum frame at the calculated swing height.

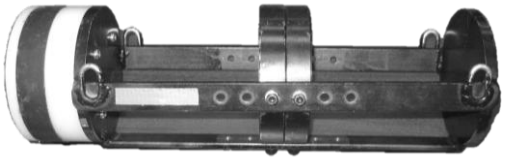

Figure 1: Pendulum frame, circular metal weights, and MEP impactor cap.

3.1.3 HYBRID III HEAD AND NECK FORM

For this experiment, a 50th percentile adult male Hybrid III head and neck form was impacted. The Hybrid III head form with mass of 4.54 ± 0.01 kg, was attached to a Hybrid III neck form with mass of 1.54 ± 0.01 kg (Fig. 2). This head and neck form is currently the most widely used and advanced human surrogate with biofidelity built into its impact response. The Hybrid III geometry and its characteristics such as head mass and location of its center of gravity was established based on cadaveric experimentation. This means that it represents human impact characteristics in terms of the essential biomechanical responses (Deng, 1989; Hubbard & McLeod, 1974).

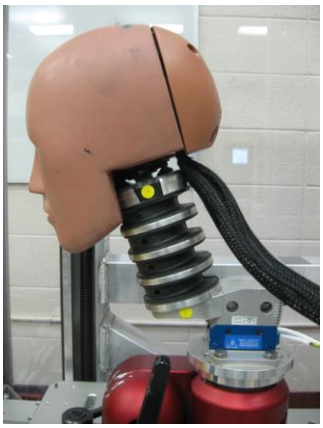

Figure 2: Hybrid III head/neck form

The dynamic response of the head form, namely the three-dimensional motion during impact, was measured using nine calibrated single-axis Endevco7264C-2KTZ-2-300 accelerometers (Endevco, San Juan Capistrano, CA), orthogonally positioned in a 3-2-2-2 array and fixed near the center of gravity of the head form (Fig. 3) (Padgaonkar et al., 1975). Angular acceleration was calculated using the first principles of rigid body dynamics and linear acceleration from the linear accelerometer orthogonal array with the following equations:

$$(1) \quad \vec{\alpha_x} = \frac{\vec{a_{zS}} - \vec{a_{zC}}}{2S} - \frac{\vec{a_{yT}} - \vec{a_{yC}}}{2T}$$

$$(2) \quad \vec{\alpha_y} = \frac{\vec{a_{xT}} - \vec{a_{xC}}}{2T} - \frac{\vec{a_{zF}} - \vec{a_{zC}}}{2F}$$

$$(3) \quad \vec{\alpha_z} = \frac{\vec{a_{yF}} - \vec{a_{yC}}}{2F} - \frac{\vec{a_{xS}} - \vec{a_{xC}}}{2S}$$

Where α_i is the angular acceleration for the component *i* (*x*, *y*, *z*) and a_{ij} is for the linear acceleration for component *i* (*x*, *y*, *z*) along the orthogonal arm *j* (S, T, F) (Padgaonkar et al., 1975). The left-hand rule was used to define the coordinate system for the head form (Walsh

et al., 2011). The positive axis is directed anteriorly towards the right ear, and caudally for the *x*, *y* and *z*, respectively (Walsh et al., 2011).

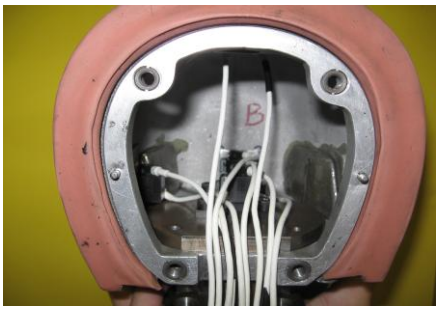

Figure 3: Orthogonally positioned 3-2-2-2 accelerometer array

3.2 TISSUE DEFORMATION

3.2.1 UNIVERSITY COLLEGE DUBLIN BRAIN TRAUMA MODEL

The three-dimensional dynamic response of the Hybrid III head form, the *x*, *y*, and *z*-axes acceleration loading curves for both linear and angular acceleration, were inputted into the University College Dublin Brain Trauma Model (UCDBTM) (Horgan & Gilchrist, 2003) for finite element analysis. The model produces brain tissue deformation corresponding to head accelerations upon impact. This model has been partially validated by comparing model responses against cadaveric experiments measuring intracranial pressure (Nahum et al., 1977) and relative brain motion (Hardy et al., 2001). Furthermore this model was validated against reconstructions of actual traumatic brain injury incidents (Doorly & Gilchrist, 2006). The head geometry of this model was determined through Computed Tomography (CT), Magnetic Resonance Imaging (MRI), and sliced contour photographs of a male cadaver (Horgan & Gilchrist, 2003). The components of this model include the scalp, a 3-layered skull, dura, CSF, pia, falx, tentorium, cerebral hemispheres, cerebellum, and brainstem. This model mathematically equates the response characteristics of neural tissue (von Mises stress,

and maximum principal strain) of various anatomical locations within the brain, accounting for their respective material properties. Table 3 & 4 summarizes the mechanical properties of the anatomical model components, which were established from previously conducted research using cadavers (Ruan, 1994; Willinger et al., 1995; Zhou et al., 1996; Kleiven & von Holst, 2002).

Table 3: Material properties for UCDBTM

Material	Young's modulus (MPa)	Poisson's ratio	Density (kg/m^3)
Scalp	16.7	0.42	1000
Cortical Bone	15000	0.22	2000
Trabecular Bone	1000	0.24	1300
Dura	31.5	0.45	1130
Pia	11.5	0.45	1130
Falx and Tentorium	31.5	0.45	1130
Brain	Hyperelastic	0.49	1040
CSF	Water	0.50	1000
Facial Bone	5000	0.23	2100

Table 4: Material characteristics of brain tissue components for UCDBTM.

Material	G_0	G_∞	Decay Constant (Gpa)	Bulk Modulus (s^{-1})
Cerebellum	10	2	80	2.19
Brain Stem	22.5	4.5	80	2.19
White Matter	12.5	2.5	80	2.19
Grey Matter	10	2	80	2.19

The behaviour of the brain tissue was modeled as viscoelastic in shear combined with large deformation theory, and the compressive behaviour of the brain is considered elastic (Horgan and Gilchrist, 2003). The shear modulus characteristics of the brain tissue modeled as viscoelastic, is shown as:

$$G(t) = G_\infty + (G_0 - G_\infty)e^{-\beta t}$$

Where G_∞, is the long term shear modulus, G_0, is the short term shear modulus, and β is the

decay factor (Horgan & Gilchrist, 2003). Modeling of the CSF was done using solid elements as low shear and high bulk modulus. The skull brain interface is represented by the models interaction between the CSF and the brain with a sliding boundary condition, thus allowing for a sliding like behaviour similar to that of water. The brain shear is modeled as hyperelastic and is represented by the following equation:

$$C_{10}(t) = 0.9C_{01}(t) = 620.5 + 1930e^{-t/0.008} + 1103e^{-t/0.15} \text{ (Pa)}$$

Where C_{10}, and C_{01} are temperature dependent material parameters, and t is seconds (Horgan & Gilchrist, 2003).

Overall the UCDBTM consists of approximately 26, 000 hexahedral elements (Horgan and Gilchrist, 2003; Horgan and Gilchrist, 2004). Visually, the results from this model are shown as a gradient of high to low deformation that is experienced throughout the brain tissue, resulting from impact (Fig. 4). The peak value of the maximum principal strain and von Mises stress will be measured within the brain and used for analysis. The von Mises stress is calculated as:

$$\sigma = \sqrt{0.5\left[(\sigma_x - \sigma_y)^2 + (\sigma_y - \sigma_z)^2 + (\sigma_z - \sigma_x)^2\right]} + \sqrt{+3\left(\tau_{xy}^2 + \tau_{yz}^2 + \tau_{zx}^2\right)}$$

where,
σ = the normal stress in a given axis;
τ = the shear stress in a given axis.

Maximum principal strain is calculated as:

$$\varepsilon 1, 2 = \frac{\varepsilon_x + \varepsilon_y + \varepsilon_z}{3} \pm \frac{\sqrt{2}}{3}\sqrt{(\varepsilon_x - \varepsilon_y)^2 + (\varepsilon_y - \varepsilon_z)^2 + (\varepsilon_z - \varepsilon_x)^2}$$

where,
εx, εy and εz = strains measured along corresponding axes.

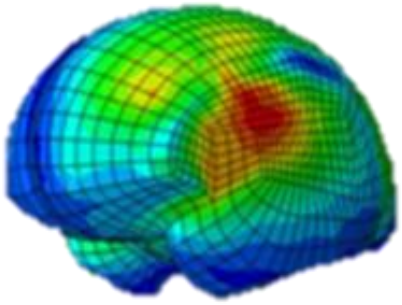

Figure 4: UCDBTM showing a gradient of high to low deformation throughout the brain.

3.3 INDEPENDENT VARIABLES

1. Inbound mass (kg): 4.3; 6.3; 8.3; 10.3; 12.3, 14.3.
2. Impact site (location and angle): centric (Side Center Gravity); non-centric (Front Boss 45° Positive Azimuth).

3.4 DEPENDENT VARIABLES

1. Kinematic response: peak resultant linear acceleration (g); peak resultant rotational acceleration (rad/s^2).
2. Brain tissue deformation: peak von Mises stress (kPa); peak maximum principal strain

3.5 RESEARCH DESIGN

To evaluate the influence of impact mass on the peak resultant linear acceleration, peak resultant angular acceleration, and tissue response characteristics within the brain, the research of this thesis comprised a fully crossed 2 x 6 balanced design (Table 5).

Table 5: Fully crossed 2 x 6 research design

	A1	**A2**	**A3**	**A4**	**A5**	**A6**
B1	A1B1	A2B1	A3B1	A4B1	A5B1	A6B1
B2	A1B2	A2B2	A3B2	A4B2	A5B2	A6B2

Legend:

Inbound mass:
A1: 4.3 kg
A2: 6.3 kg
A3: 8.3 kg
A4: 10.3 kg
A5: 12.3 kg
A6: 14.3 kg

Impact location:
B1: centric (SCG)
B2: non-centric (FBPA)

3.5.1 PROCEDURES

The influence of inbound mass on the dynamic impact response of the Hybrid III headform and the tissue deformation response, at varying impact conditions was examined. The Hybrid III head form was impacted 5 times under each impact condition. Impacts were performed at two impact locations in accordance with the University of Ottawa Testing Protocol (Walsh et al., 2011) defined in Table 6 (Appendix A), and with six impact masses. The inbound masses were chosen as they encompass a range of inbound masses that are seen with sport impacts (Atha, Yeadon, Sadover, & Parsons, 1985; Zazryn et al., 2006; Viano et al., 2005; Walilko, Viano & Bir, 2005; Smith & Hamill, 1986). Each impact was executed at a velocity of 4.0 m/s for a total of 60 impacts. For this study, a low impact velocity was chosen to avoid material saturation from impacts to the bare headform. Higher velocity impacts seen within sport typically involve head protection.

Table 6: University of Ottawa Testing Protocol Five (uOTP5) impact location specifications.

Impact Location	Site	Angle
Side Center of Gravity (Centric)	Right intersection of the coronal and absolute transverse plane	Perpendicular to the head form surface, no vertical or horizontal rotation was applied to the vector
Front Boss 45° Positive Azimuth (Non-centric)	Midpoint between the anterior mid-sagittal and right coronal planes in absolute transverse plane	A 45° rotation of the head form in the transverse plane

3.5.2 DATA COLLECTION AND FILTERING

The velocity of the pendulum impactor prior to impacting the head form was measured using a High Speed Imaging PCI-512 Fastcam running at 2 kHz and Photron Motion Tools computer software (Photron, San Diego CA) for consistency. Signals from the nine accelerometers were sampled at 20 kHz and filtered through a 1000 Hz low pass Butterworth filter using SAE J211 Class 1000 protocol (SAE, 2007). Data collection was triggered upon a 3 g threshold reached by any one of the accelerometers and was collected for duration of 15 ms. Signals from the accelerometers were passed through TDAS Pro Lab module (DTS, Calabasas, CA), before being processed with TDAS software. Data analysis and filtering was done using BioProc3, software developed by Dr. D.G.E. Robertson, University of Ottawa (2008).

3.5.3 STATISTICAL ANALYSIS

The purpose of this research thesis was to describe the influence of impact mass on the dynamic impact response and brain tissue response. A one-way analysis of variance (ANOVA) was performed for each of the four dependent variables for each impact condition to determine the effects of a change in inbound mass. A significance level of $\alpha = 0.05$ was set, and a post hoc Tukey was performed when significance was found. Therefore, the

statistical analysis for this thesis consisted of a total of 8 one-way ANOVA to meet its objectives. All statistical analyses were performed using SPSS 18.0 software (SPSS Inc., Chicago IL, USA).

CHAPTER 4. RESULTS

To determine the influence of inbound mass on the dependent variables, eight ANOVA were completed. The following section presents the results for both the dynamic impact testing, and finite element analysis of the brain tissue deformation.

4.1 DYNAMIC IMPACT RESULTS

Table 7 displays the mean peak linear and angular accelerations of a Hybrid III head form for each inbound mass tested. These are the results from impacts performed at a velocity of 4.0 m/s to a centric (SCG) and non-centric (FBPA) location using six different inbound masses. The means and standard deviations were determined from five trial impacts performed for each condition. Results for each impact trial can be found in Appendix B.

Table 7: Mean peak dynamic response (± 1 standard deviation) of the hybrid III head form resulting from impacts with six inbound masses performed at 4.0 m/s to a centric and non-centric impact location.

	Centric (Side CG)		**Non-Centric (Front Boss PA)**	
Inbound Mass (kg)	**Linear Acc. (g)**	**Angular Acc. (krad/s^2)**	**Linear Acc. (g)**	**Angular Acc. (krad/s^2)**
4.3	177.8 ± 1.9	15.2 ± 0.2	158.7 ± 6.8	18.4 ± 0.8
6.3	199.4 ± 2.3	16.1 ± 0.2	180.7 ± 4.1	18.8 ± 0.7
8.3	210.5 ± 0.8	17.0 ± 0.1	191.6 ± 1.8	17.8 ± 0.5
10.3	228.4 ± 5.9	18.0 ± 0.3	197.6 ± 3.4	18.2 ± 0.7
12.3	228.4 ± 3.1	17.9 ± 0.2	200.4 ± 3.9	18.8 ± 1.4
14.3	229.6 ± 2.6	17.5 ± 0.6	226.5 ± 0.5	19.9 ± 0.2

4.1.1 ANALYSIS OF VARIANCE (ANOVA)

One-way ANOVA was conducted for each dynamic response variable at two impact locations to determine the effects that inbound mass has on the mean peak linear and angular accelerations at both a centric and a non-centric impact location. A change in inbound mass was found to have a significant effect on peak linear acceleration for centric ($F(5, 24) = 217.55$, $p<0.0005$) and non-centric ($F(5, 24) = 161.98$, $p<0.0005$) impact locations. Significance was also found for peak angular acceleration for centric ($F(5, 24) = 52.51$, $p<0.0005$) and non-centric ($F(5, 24) = 4.18$, $p=0.007$) impacts. Therefore the four null hypotheses regarding the effects of inbound mass on the dynamic response variables were all rejected.

4.1.1.1 CENTRIC IMPACT LOCATION

Tukey post hoc tests revealed that mean peak linear and mean peak angular accelerations resulting from an inbound mass of 10.3 kg, 12.3 kg and 14.3 kg were not significantly different from one another (Fig. 5, 6). In addition, no significant difference in mean peak angular acceleration between an inbound mass of 8.3 kg and 14.3 kg was observed.

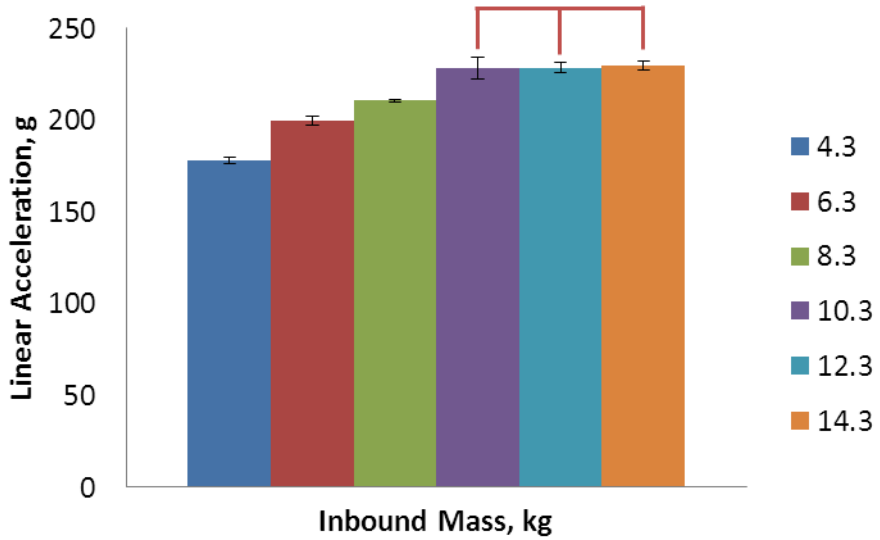

Figure 5: Mean peak linear accelerations resulting from six inbound masses at a centric (SCG) impact location.

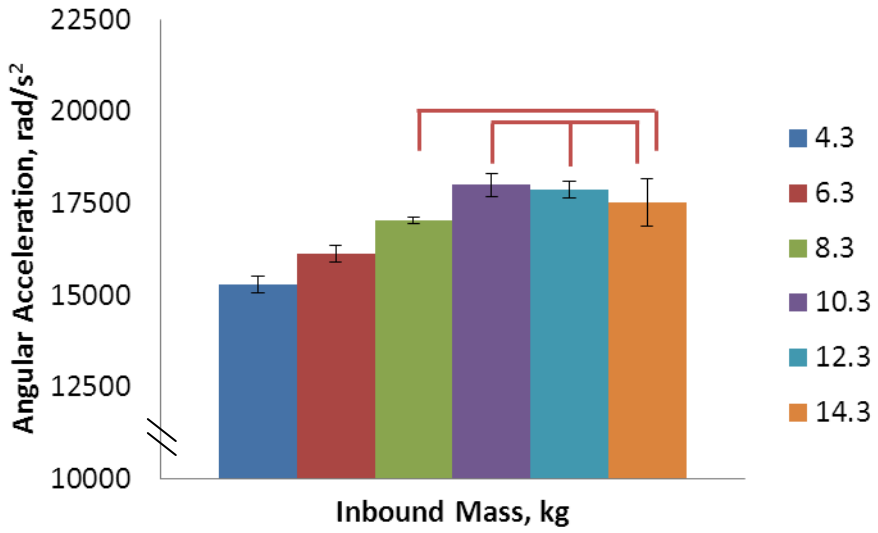

Figure 6: Mean peak angular accelerations resulting from six inbound masses at a centric (SCG) impact location.

4.1.1.2 NON-CENTRIC IMPACT LOCATION

Significant differences in the mean peak linear accelerations resulting from a non-centric impact were found between all inbound masses tested excluding those between an 8.3 kg and 10.3 kg mass, and between a 10.3 kg and 12.3 kg inbound mass (Fig. 7). For mean peak angular accelerations, significant differences were found between an inbound mass of 8.3 kg and 14.3 kg, and also between angular accelerations resulting from inbound masses of 10.3 kg and 14.3 kg (Fig. 8).

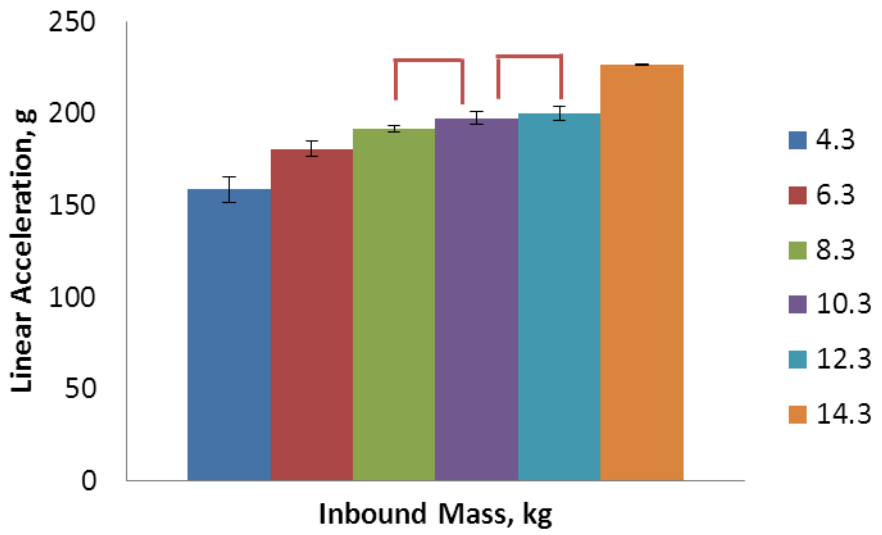

Figure 7: Mean peak linear accelerations resulting from six inbound masses at a non-centric (FBPA) impact location.

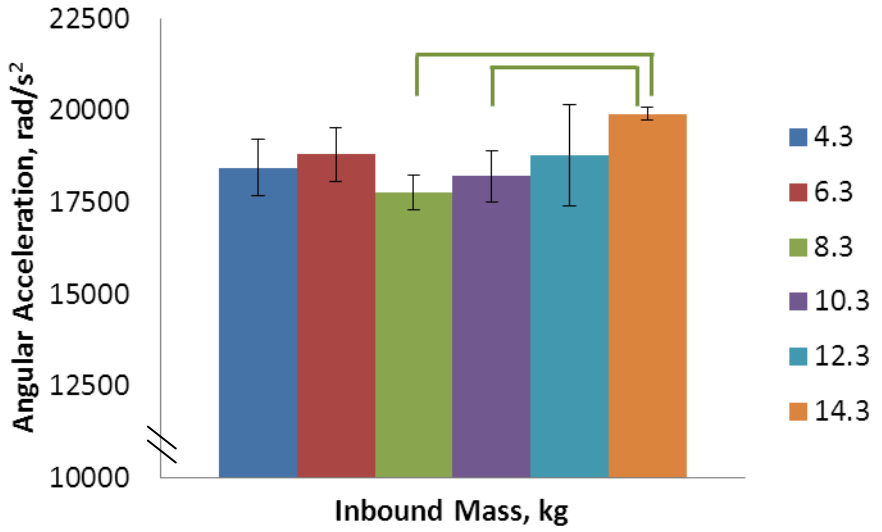

Figure 8: Mean peak angular accelerations resulting from six inbound masses at a non-centric (FBPA) impact location.

4.2 BRAIN DEFORMATION RESULTS

Table 8 displays the mean peak maximum principal strain and von Mises stress for each inbound mass tested. These are the results obtained from finite element analysis using the dynamic response data from impacts performed to a centric (SCG) and non-centric (FBPA) impact location at a velocity of 4.0 m/s using six different inbound masses. The means and

standard deviations were determined from five trial impacts performed for each condition. Results for each impact trial can be found in Appendix C.

Table 8: Mean peak brain tissue deformation metrics (± 1 standard deviation) as determined from finite element analysis resulting from impacts with six inbound masses performed at 4.0 m/s to a centric and non-centric impact location.

	Centric (Side CG)		**Non-Centric (Front Boss PA)**	
Inbound Mass (kg)	**maximum principal strain**	**von Mises stress (kPa)**	**maximum principal strain**	**von Mises stress (kPa)**
4.3	0.285 ± 0.009	10.1 ± 0.4	0.499 ± 0.024	19.9 ± 1.0
6.3	0.304 ± 0.004	11.1 ± 0.2	0.536 ± 0.017	21.3 ± 0.8
8.3	0.315 ± 0.009	11.3 ± 0.2	0.493 ± 0.017	19.3 ± 0.8
10.3	0.330 ± 0.016	12.2 ± 0.4	0.527 ± 0.012	20.6 ± 0.6
12.3	0.326 ± 0.016	12.1 ± 0.3	0.562 ± 0.042	22.1 ± 2.0
14.3	0.325 ± 0.009	11.7 ± 0.5	0.516 ± 0.016	19.9 ± 0.7

4.2.1 ANALYSIS OF VARIANCE (ANOVA)

One-way Analysis of Variance (ANOVA) was conducted for each brain deformation variable at two impact locations to determine the effects that inbound mass has on the mean peak maximum principal strain and von Mises stress at both a centric and a non-centric impact location. A change in inbound mass was found to have a significant effect on peak maximum principal strain for centric ($F(5, 24) = 11.04$, $p<0.0005$) and non-centric ($F(5, 24) = 5.87$, $p =0.001$) impact locations. Significance was also found for peak von Mises stress for centric ($F(5, 24) = 24.01$, $p<0.0005$) and non-centric ($F(5, 24) = 4.62$, $p=0.004$) impacts. Therefore the four null hypotheses concerning the effects of inbound mass on brain deformation were all rejected.

4.2.1.1 CENTRIC IMPACT LOCATION

Results for the centric impact location found significant differences for resulting mean peak maximum principal strains between an inbound mass of 4.3 kg and 8.3 kg, 10.3 kg, 12.3 kg, and 14.3 kg masses, and between mean maximum principal strains from 6.3 kg inbound mass and 10.3 kg inbound mass (Fig. 9). Tukey post hoc tests showed that mean peak von Mises stress resulting from an inbound mass of 10.3 kg, 12.3 kg and 14.3 kg were not significantly different from one another. In addition, mean peak von Mises stress results between an inbound mass of 6.3 kg and 8.3 kg, 6.3 kg and 14.3 kg, and finally between 8.3 kg and 14.3 kg were not significantly different (Fig. 10).

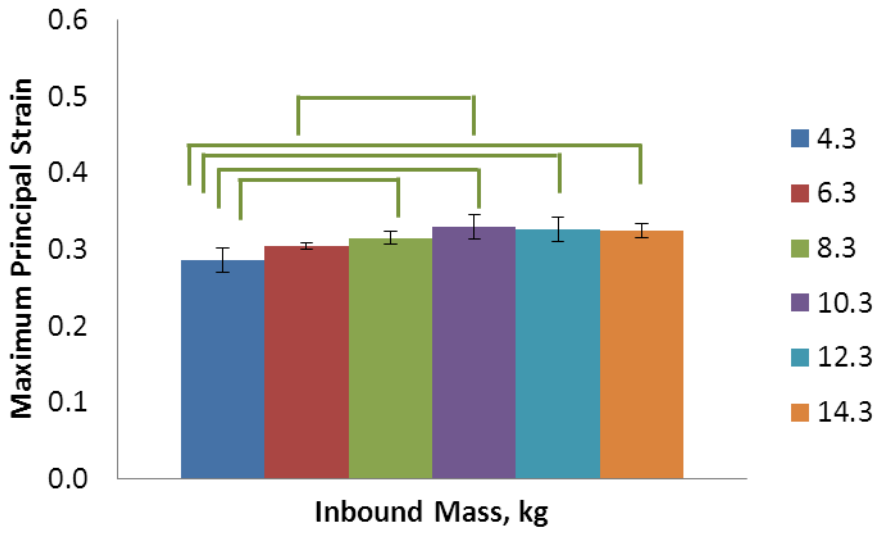

Figure 9: Mean peak maximum principal strain resulting from six inbound masses at a centric (SCG) impact location.

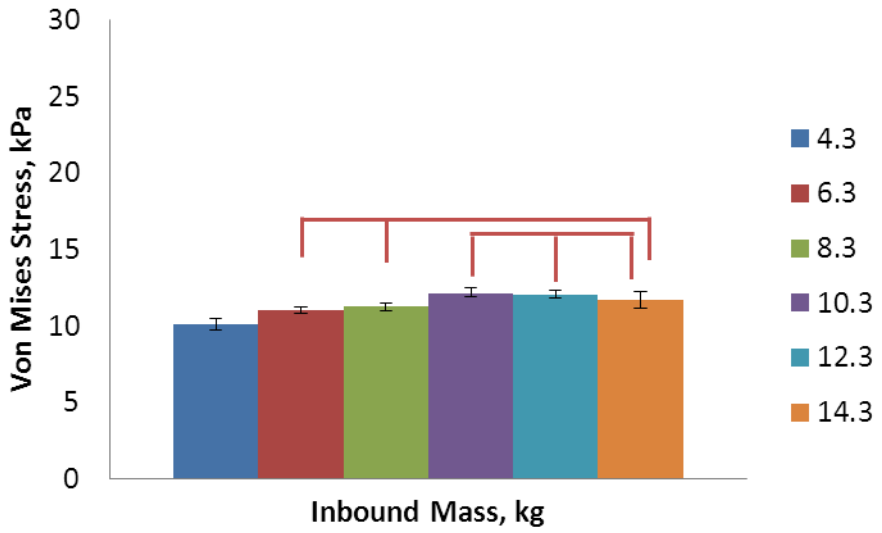

Figure 10: Mean peak von Mises stress resulting from six inbound masses at a centric (SCG) impact location.

4.2.1.2 NON- CENTRIC IMPACT LOCATION

Significant differences were found for mean peak maximum principal strains and mean peak von Mises stress resulting between inbound masses of 4.3 kg and 12.3 kg, 8.3 kg and 12.3 kg, and between mean results from 12.3 kg and 14.3 kg inbound mass impacts (Fig. 11, 12).

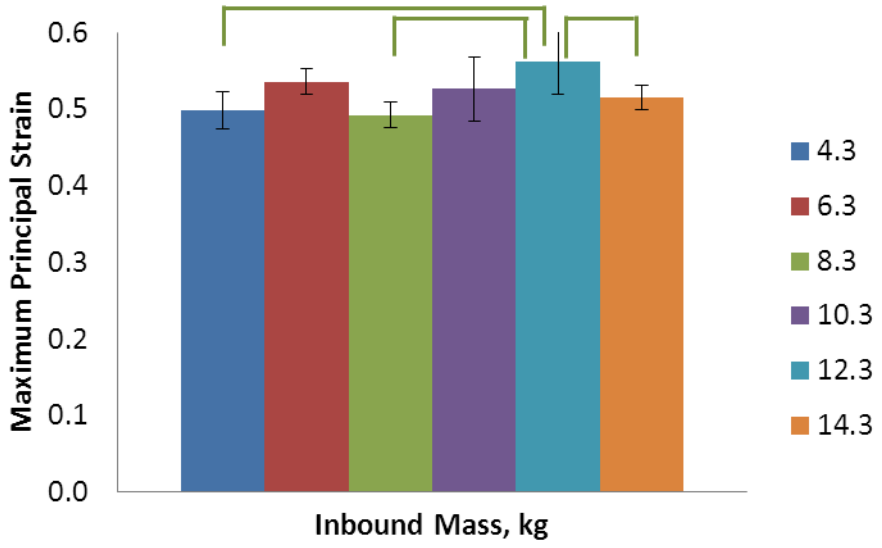

Figure 11: Mean peak maximum principal strain resulting from six inbound masses at a non-centric (FBPA) impact location.

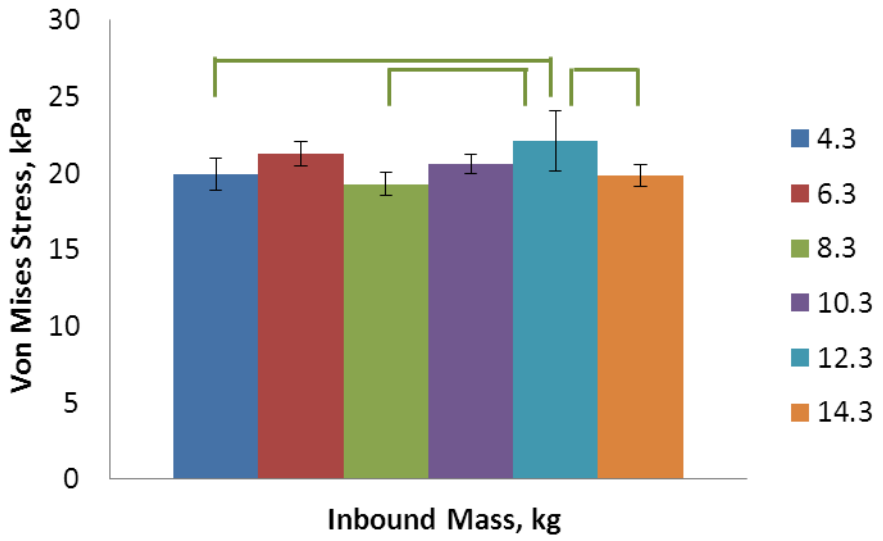

Figure 12: Mean peak von Mises stress resulting from six inbound masses at a non-centric (FBPA) impact location.

The resulting values for mean peak linear acceleration show an increase as the inbound mass of the impact was increased. However, this trend was not observed with mean peak angular accelerations resulting from an increase in inbound mass. Moreover brain deformation resulted in values of a similar trend to peak angular acceleration as the inbound mass was increased. Overall statistical analysis revealed that a change in the inbound mass of an impact to the head has a significant effect on the resulting dynamic impact and brain tissue responses. Significant differences were observed for both mean peak linear and mean peak angular accelerations for both a centric and non-centric impact conditions. Further, both mean peak maximum principal strain and mean peak von Mises stress showed significant differences from a change in inbound mass for a centric and a non-centric impact conditions. However, post hoc analysis discovered that the specific areas of significance did vary among each dependent variable and between centric and non-centric impacts.

CHAPTER 5. DISCUSSION

Reconstructions of head impact events have become a widely used method for establishing biomechanical mechanisms responsible for injury (Zhang et al., 2003; 2004; Kleiven, 2003; Pellman et al., 2003; Willinger & Baumgarthner, 2003). An understanding of how the various characteristics of an impact influence the resulting head and brain injuries is necessary in order to derive associated injury risks from impact reconstructions. This study has demonstrated that variation in inbound mass can have a significant effect on the dynamic response of the head, and subsequent damage to neural tissue.

The results for peak linear and peak angular accelerations do not follow the same trend as the inbound mass is increased. Peak linear accelerations follow a linear trend increasing as the inbound mass gets higher. On the other hand, peak angular accelerations did not show this same pattern as the inbound mass was changed. A notable aspect regarding the peak angular accelerations is the high standard deviations observed between trial impacts. The impact dynamics of the pendulum system that was used for this research could have had an influence on these phenomena. The non-centric site was very close to the front edge of the head form (Walsh et al., 2011) whereas for the centric impact site, the pendulum hit the middle of the head form providing more of a follow through, and possibly resulting in a more complete transfer of momentum.

Linear accelerations for the centric impact location show stabilization from an inbound mass of 10.3 to 14.3 kg. This could indicate saturation in the compliance, or energy absorption, of the materials involved in the impact, namely the Hybrid III head and neck form and MEP impactor cap. This plateau was not observed for the non-centric impact, though these impacts

did not reach the same acceleration of approximately 228 g, even with the highest tested mass.

Peak angular accelerations and the peak deformation variables for both the centric and non-centric impacts revealed a similar trend with the increase of inbound mass. This is in accordance with other studies that have discovered that the angular response of the head form may have a more primary influence on brain deformation. This was realized in literature that has found high positive correlations between these two response variables resulting from helmeted impacts (Yang & King, 2003; Forero Rueda et al., 2010; Post, Oeur, Hoshizaki et al., 2011), as well as research that associates both angular acceleration and brain deformation with concussion type injuries (Gennarelli et al., 1982; Zhang et al., 2004).

In addition, the results from this experiment suggest that the inbound mass of an impact influences these dependent variables differently depending on the location of the impact. This finding was consistent with previous research that shows variation occurs in the head kinematics and brain tissue response by changing the parameters of the impact (Gennarelli et al., 1982; 1987; Zhang, Yang & King, 2001; Kleiven, 2003; Pellman et al, 2003; Willinger & Baumgartner, 2003). To compare centric and non-centric impacts in terms of proportion increase within the response variables due to increasing inbound mass, percentage difference calculations were completed. The percentage differences between centric and non-centric impacts for peak linear and angular accelerations ranged from 1.3 to 14.5 % and 1.1 to 18.7 %, respectively. Interestingly though, the percentage differences in peak tissue deformation variables were considerably higher. Percentage differences between centric and non-centric impacts for peak maximum principal strain and peak von Mises stress ranged from 44.1 to 55.3 % and 51.6 to 65.4 %, respectively. Please refer to Appendix D for percentage differences for all masses and dependent variables. This disproportion may be explained by

considering the shape of the individual curves created by the impact, within each of the three axes (Post et al., 2010). The brain model uses an integration of these acceleration time curves, rather than peak resultant values, when determining brain tissue responses.

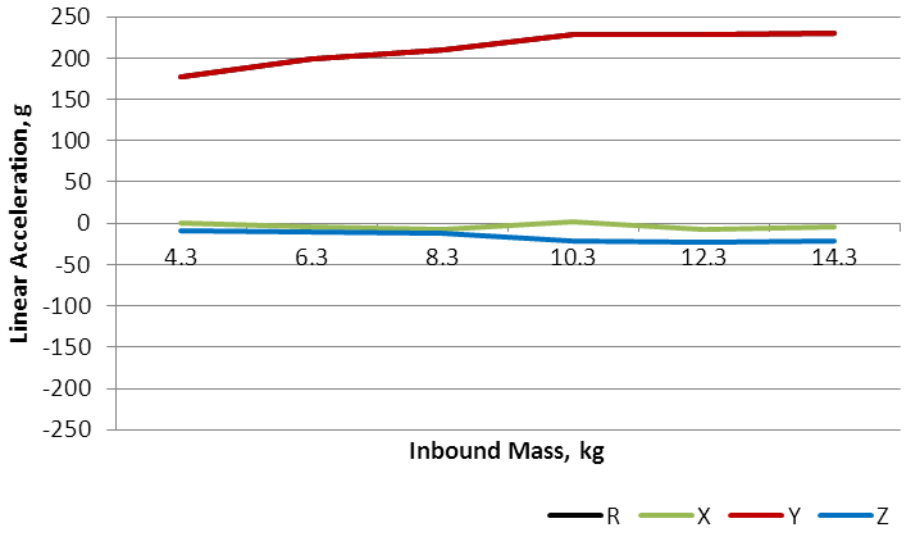

Figure 13: Peak linear accelerations within the x (green), y (red), and z (blue) axes across six inbound masses from the centric (SCG) impact location. Peak resultant (black) follows the y axis.

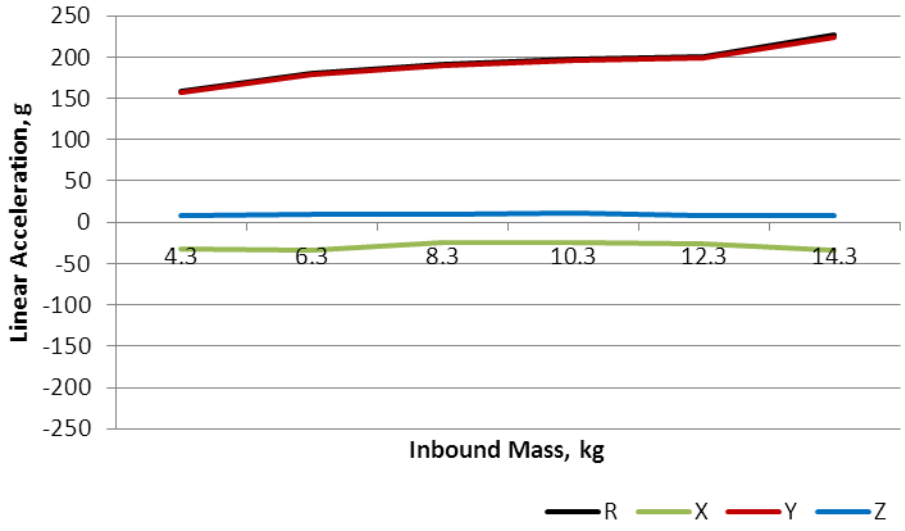

Figure 14: Peak linear accelerations within the x (green), y (red), and z (blue) axes across six inbound masses from the non-centric (FBPA) impact location. Peak resultant (black) follows the y axis.

Examining the impact from this standpoint, results showed that similar single axis responses are similar for linear acceleration between centric and non-centric conditions (Fig. 13, 14),

however, the non-centric impacts created higher angular acceleration about the z-axis. Also the centric impact location, on the side of the head, produced higher values within the x-axis, representing a slight trade off (Fig. 15, 16). This occurrence was not observed in view of the peak resultant dynamic response alone.

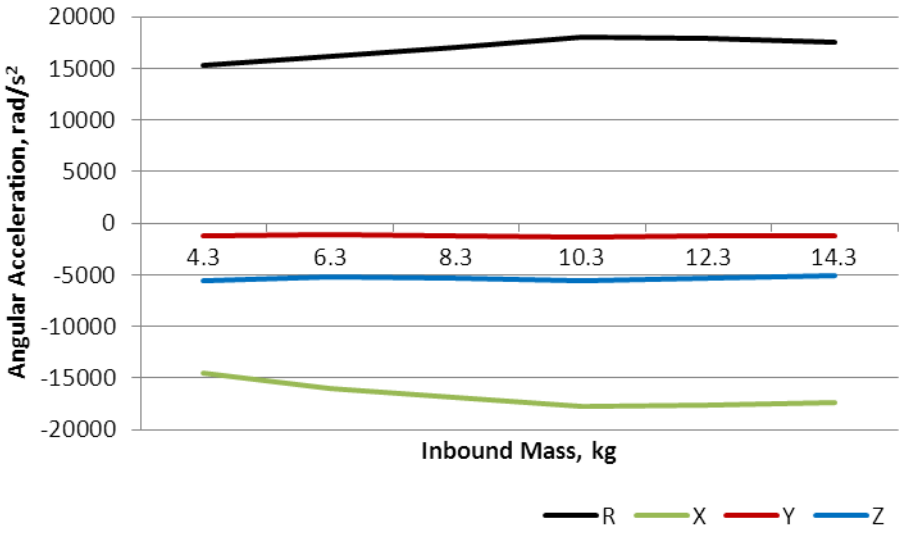

Figure 15: Peak angular accelerations within the x, y, and z axes across six inbound masses from the centric (SCG) impact location.

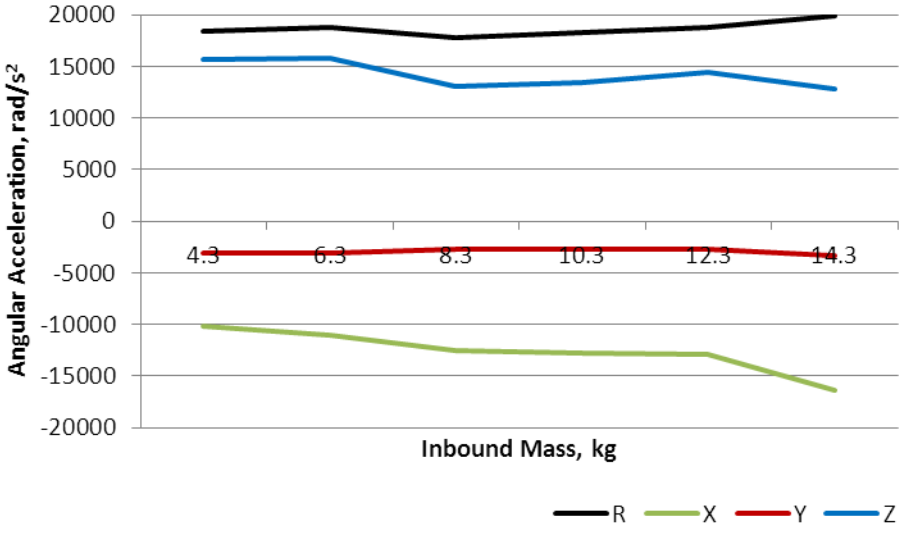

Figure 16: Peak angular accelerations within the x, y and z axes across six inbound masses from the non-centric (FBPA) impact location.

Non-centric impacts have been shown to create a more rotation dominant response, or angular acceleration of the head (Walsh et al., 2011). This method was demonstrated by Viano and associates (2005), where boxing punches created proportionately higher head rotational acceleration when compared to NFL impacts, even when a similar inertial force of the head was created from the impact. The results from this study support this finding where the peak maximum principal strain and von Mises stress values were much higher for the non-centric impact location. This indicates that inbound mass has a varied influence on brain deformation depending on the head location of the impact. Moreover, peak accelerations may not represent the severity of brain deformation when impacts to the head are non-centric.

The findings from this study are supported by previous research within the sport domain that has demonstrated that an increase in effective mass of an impact can create higher risks to head injury (Smith & Hamill, 1986; Pellman et al., 2003; Walilko, Viano & Bir, 2007). Both Smith and Hamill (1986), and Walilko and colleagues (2007) reported that a high effective mass of a boxing punch was a main predictor of generating injurious outcomes. In addition, Shewchenko and colleagues' (2005) study on heading a soccer ball, showed that as the mass of the ball increased, so too did the head response measures, including linear acceleration, angular acceleration and HIC. Furthermore, the struck player in player-to-player impacts commonly seen in football is at higher risks of injury, due to the higher effective mass generated by the striking player's impact (Pellman et al., 2003).

It must be noted that the impacts in this study were performed on a bare head form meaning there was no helmet to absorb energy and lessen the severity. Therefore, an aspect worth noting is that even the lowest inbound mass of 4.3 kg was able to produce high values for all

of the dependent variables. These results may speak to sports such as boxing where protective headgear is not worn and where head injuries are prevalent, concussion being amongst the most common (Zazryn et al, 2001).

CHAPTER 6. CONCLUSION, CONTRIBUTIONS, AND FUTURE WORK

6.1 CONCLUSION

Overall, all eight null hypotheses were rejected. The results from this thesis indicate that the inbound mass of an impact had a significant effect on the dynamic response of the head form and brain tissue deformation.

6.2 CONTRIBUTIONS

This experiment was the first to relate the inbound mass of an impact to the resulting dynamic response of the Hybrid III head form, and to the corresponding deformation to brain tissue. It was successful in indicating that consideration of this impact variable is of significant importance for injury reconstruction and associated risks to injury. This study has provided a better understanding of the effects of inbound mass and has expanded the knowledge concerning how the variation of impact characteristics can change the dynamic and brain tissue response. Ultimately this leads us to better understand reconstruction and interaction for helmet design and protection.

6.3 FUTURE WORK

Due to the growing concern of concussion injuries in sport and the vast discrepancy between the symptomology, severity of injury, and recovery time and return to play, research interest on this subject will not be soon be exhausted. Technological advancement in finite element models has provided an understanding of the brain tissue response and associations with mTBI. As the effects of impact characteristics on global brain tissue deformation is important, further investigation on the damage to, and sensitivity of specific brain regions is

an important future direction as it may lead to more insight on properly diagnosing, treating, and preventing head and brain injures.

REFERENCES

Adams, J.H., Graham, D.I. & Gennarelli, T.A. (1981). Acceleration induced head injury in the monkey: II. *Neuropathology, 7*, 26-28.

Adams, J.H., Graham, D.I., Murray, L.S. & Scott, G. (1982). Diffuse axonal injury due to nonmissile head injury in humans: an analysis of 45 cases. *Annals of Neurology, 12*(6), 557-563.

Al-Bsharat, A.S., Hardy, W.N., Yang, K.H., Khalil, T.B., Tashman, S., & King, A.I. (1999). Brain/skull relative displacement magnitude due to blunt head impact: New experimental data and model. *Proceedings of the 43rd Stapp Car Crash Conference*, San Diego, California, USA, SAE 99SC22.

Anderson, R.W., Brown, C.J., Blumbergs, P.C., McLean, A.J. & Jones, N.R. (2003). Impact mechanics and axonal injury in a sheep model. *Journal of Neurotrauma, 20,* 961-974.

Atha, J., Yeadon, M.R., Sadover, J. & Parsons, K.C. (1985). The damaging punch. *British Medical Journal, 291*, 1756-1757.

Avalle, M., Belingardi, G., & Montanini, R. (2001). Characterization of polymeric structural foams under compressive impact loading by means of energy-absorption diagram. *International Journal of Impact Engineering, 25*. 455-472.

Bailes, J.E. & Cantu, R.C. (2001). Head injury in athletes. *Neurosurgery, 48*(1), 26-45.

Bain, A. & Meaney, D. (2000). Tissue-level thresholds for axonal damage in an experimental model of central nervous system white matter injury. *Journal of Biomechanics, 122*, 615-622.

Barth, J.T., Freeman, J.R., Broshek, D.K. & Varney, R.N. (2001). Acceleration-deceleration sport-related concussion: The gravity of it all. *Journal of Athletic Training. 36*, 253-256.

CAN/CSA-D113.2-M89 Cycling Helmets. A National Standard for Canada (Reaffirmed 2004). May 1996.

Casson, I.R., Viano, D.C., Powell, J.W. & Pellman, E.J. (2010). Twelve years of national football league concussion data. Sports Health: *A Multidisciplinary Approach, 2*(6), 471-484.

Carpenter, M.B. (1991). Core text of Neuroanatomy (4th ed.). Williams & Wilkins, Baltimore, Maryland.

Delaney, J.S., Lacroix, V.J., Leclerc, S. & Johnston, K.M. (2002). Concussions among university football and soccer players. *Clinical Journal of Sports Medicine, 12*, 331-338.

Deng, Y. (1989). Anthropomorphic dummy neck modeling and injury considerations. *Accident Analysis & Prevention*, 21(1), 85-100.

Duma, S.M., Manoogian S.J., Bussone, W.R. et al. (2005). Analysis of real-time head accelerations in collegiate football players. *Clinical Journal of Sports Medicine, 15,* 3–8.

Doorly, M.C. & Gilchrist, M.D. (2006). The use of accident reconstruction for the analysis of traumatic brain injury due to head impacts arising from falls. *Computer Methods in Biomechanics and Biomedical Engineering, 9*(6), 371-377.

Flik, K., Lyman, S. & Marc, R.G. (2005). American collegiate men's ice hockey: an analysis of injuries. *American Journal of Sports Medicine, 33,* 183-187.

Forero Rueda, M.A., Cui, L. & Gilchrist, M.D. (2010). Finite element modeling of equestrian helmet impacts exposes the need to address rotational kinematics in future helmet designs. *Computer Methods in Biomechanics and Biomedical Engineering, 1,* 1-11.

Gadd, C. W. (1966). Use of a weighted-impulse criterion for estimating injury hazard. Proceeding in the *10th Stapp Car Crash Conference*. SAE Paper No. 660793.

Galbraith, J.A., Thibault, L.E. & Matteson, D.R. (1993). Mechanical and electrical responses of the squid giant axon to simple elongation. *Journal of Biomechanical Engineering, 115*, 13-22.

Gardner, E. (1975). *Fundamentals of Neurology, A Psychophysiological Approach (6th ed.).* W.B. Saunders Company, Philadelphia, PA.

Gennarelli, T.A, Thibault, L.E. & Ommaya, A.K. (1972). Pathophysiological Responses to Rotational and Translational Accelerations of the Head, SAE Paper No. 720970, in: *16thh Stapp Car Crash Conference.*, Society of Automotive Engineers, p. 296-308.

Gennarelli, T.A., Abel, J.M., Adams, H. & Graham, D. (1979). Differential Tolerance of Frontal and Temporal Lobes to Contusion Induced by Angular Acceleration.

Gennarelli, T.A., Thibault, L.E., Adams, H., Graham, D.I., Thompson, C.J. & Marcincin, R.P. (1982). Diffuse Axonal Injury and Traumatic Coma in the Primate. *Annals of Neurology, 12*(6), 564-574.

Gennarelli, T.A., Thibault, L., Tomei, G., Wiser, R., Graham, D. & Adams, J. (1987). Directional dependence of axonal brain injury due to centroidal and non-centroidal acceleration. Proceedings in the 31st *Stapp Car Crash Conference,* p. 49-53. Society of Automotive Engineers, Warrendale, Philadelphia.

Gimbel, G. & Hoshizaki, T.B. (2008). Compressive properties of helmet materials subjected to dynamic impact loading of various energies. *European Journal of Sport Science, 8*(6), 241-249.

Goldsmith, W. & Plunkett, J. (2004). A biomechanical analysis of the causes of traumatic brain injury in infants and children. *The American Journal of Forensic Medicine and Pathology, 25*, 89-100.

Gordon, K.E., Dooley, J.M. & Wood, E.P. (2006). Descriptive epidemiology of concussion. *Pediatric Neurology, 34*, 376-378.

Greenwald, R.M., Gwin, J.T., Chu, J.J. & Crisco, J.J. (2008). Head impact severity measures for evaluating mild traumatic brain injury risk exposure. *Neurosurgery, 62*(4), 789-798.

Gurdjian, E.S., Lissner, H.R., Latimer, F.R., Haddad, B.F. & Webster, J. E. (1953). Quantitative Determination of Acceleration and Intracranial Pressure in Experimental Head Injury. *Neurology, 3*(6), 417-423.

Gurdjian, E.S., Webster, J.E. & Lissner, H.R. (1958). Mechanism of scalp and skull injuries, concussion, contusion and laceration. *Journal of Neurosurgery, 15*(2), 125-128.

Gurdjian, E.S., Roberts, V.L. & Thomas, L.M. (1966). Tolerance curves of acceleration and intracranial pressure and protective index in experimental head injury. *Journal of Trauma, 6*(5), 600-605.

Gurdjian, E.S. (1975). Re-evaluation of the biomechanics of blunt impact injury of the head. *Surgery, Gynecology & Obstetrics, 140*(6), 845-850.

Gurdjian, E.S. (1975). Impact head injury: *Mechanistic, clinical and preventative correlations.* Springfield, IL: Charles C Thomas.

Hardy, W.N., Foster, C.D., Mason, M.J., Yang, K.H. & King, A.I. (2001). Investigation of head injury mechanisms using neutral density technology and high-speed biplanar X-ray. *Proceedings of the 45th Stapp Car Crash Conference*. San Antonio, TX, pp. 337-368.

Harrell, R.M., Weinhold, P.S., Yu, B. & Kirkendall, D.T. (2004). Modelling the Impact of heading: influence of inflation pressure, contact mass, ball size and velocity. *Journal of Sports Sciences, 22*(6), 489-490

Hodgson, V.R. (1967). Tolerance of the facial bones to impact. *American Journal of Anatomy, 120*, 113-122.

Hodgson, V.R. & Thomas, T.B. (1979). Acceleration induced shear strains in a monkey brain hemisection, SAE Paper No. 791023, in: 23rd Stapp Car Crash Conference, *Society of Automotive Engineers*.

Hodgson, V.R., Thomas, L.M. & Khalil, T.B. (1983). The role of impact location in reversible cerebral concussion, SAE Paper No. 831618, in: 27th Stapp Car Crash Conference, *Society of Automotive Engineers*, 225-240.

Holbourn, A.H. (1943). Mechanics of head injuries. *Lancet, 2*, 438-441.

Horgan, T. (2005). A Finite Element Model of the Human Head for use in the Study of Pedestrian Accidents. PhD Thesis. University College Dublin.

Horgan, T. & Gilchrist, M. (2003). The creation of three-dimensional finite element models for simulating head impact biomechanics. *International Journal of Crashworthiness, 8*(4), 353-366.

Hoshizaki, T.B. & Brien, S.F. (2004). The science and design of head protection in sport. *Neurosurgery, 55*, 956-967.

Hubbard, R. & McLeod, G. (1974). Definition and development of a crash dummy head. In: *Proceedings of the 18th Stapp Car Crash Conference*, Ann Arbor MI, USA, SAE paper 741193.

Iverson, G.L., Lange, R.T., Brooks, B.L. & Rennison, V.L.A. (2010). "Good Old Days" Bias Following Mild Traumatic Brain Injury. *The Clinical Neuropsychologist, 24*, 177-37.

King, A.I., Yang, K.H., Zhang, L. & Hardy, W. (2003). Is head injury caused by linear or angular acceleration? *IRCOBI Conference*, Lisbon, Portugal, pp.1-12.

Kleiven, S. (2002). *Finite Element Modeling of the Human Head*. PhD Thesis.

Kleiven, S. (2003). Influence of impact direction to the human head in prediction of subdural haematoma. *Journal of Neurotrauma, 20*(4), 365-379.

Kleiven, S. (2007). Predictors for traumatic brain injuries evaluated through accident reconstruction. *Stapp Car Crash Journal, 51*, 1-35.

Kleiven, S. & Hardy, W. (2002). Correlation of an FE model of the human brain with experiments on localized motion of the brain – consequences for injury prediction. *Stapp Car Crash Journal, 46*, 123-144.

Kleiven, S. & von Holst, H. (2002). Consequences of head size following trauma to the human head. *Journal of Biomechanics, 35*, 153-160.

Leclerc, S., Lassonde, M., Delaney, J.S., Lacroix, V.J. & Johnston, K.M. (2001). Recommendations for Grading of Concussion in Athletes. *Journal of Sports Medicine, 31*(8), 629-636.

McIntosh, T.K., Smith, D.H., Meaney, D.F., Kotapka, M.J., Gennarelli, T.A. & Graham, D.I. (1996). Neuropathological sequelae of traumatic brain injury: relationship to neurochemical and biochemical mechanisms. *Laboratory Investigation*, 74, 315-342.

Meaney, D.F. (1991). *The biomechanics of acute subdural haematoma in the subhuman primate and man.* Ph.D. Dissertation, University of Pennsylvania, Philadelphia, PA.

Meaney, D.F. & Smith, D.H. (2011). Biomechanics of concussion. *Clinical Sports Medicine, 30*, 19-31.

Meehan, W.P. (2011). Medical therapies for concussion. *Clinical Sports Medicine, 30*, 115-124.

Montgomery, D.L. (2006). Physiological profile of professional hockey players – a longitudinal comparison. *Journal of Applied Physiology Nutrition and Metabolism, 31*, 181-185.

Nahum, A.M., Smith, R.W. & Ward, C. C. (1977). Intracranial pressure dynamics during head impact. Procedures of the 21st *Stapp Car Crash Conference*, SAE paper no. 770922.

Newman, J.A. (1986). A Generalized Acceleration Model for Brain Injury Threshold. International IRCOBI conference, 121-131.

Newman, J.A. (1993). "Biomechanics of Human Trauma: Head Protection," in Accidental Injury Biomechanics and Prevention. Springer Verlag: New York, p 292-310.

Newman, J.A. et al. (2000). A proposed new biomechanical head injury assessment function – a maximum power index, in: *44th Stapp Car Crash Conference*, SAE Paper No. 2000-01-SC16.

Newman, J. (2006). A proposal for ASTM F08-53's consideration – A new severity index NSI for helmet impact assessment. NBEC, Edmonton, Canada, 1-9.

Neyer, R. (2001). *A matter of size*. In Building the elite athlete. Scientific American, 14-15.

NOCSAE 001-06m07 (2007). National Operating Committee on Standards for Athletic Equipment (2006). Standard drop test method and equipment used in evaluating the performance characteristics of protective headgear. *NOCSAE DOC (ND) 001-06m07*.

Nusholtz, G.S., Melvin, J.W. & Alem, N. M. (1979) *Head Impact Response Comparisons of Human Surrogates*. Biomechanics of Impact Injury and Injury Tolerances of the Head-Neck Complex.

Ommaya, A.K. & Hirsch, A.E. (1971). Tolerances for cerebral concussion from head impact and whiplash in primates. *Journal of Biomechanics, 4*, 13-21.

Ommaya, A.K., Hirsch, A.E., Harris, E., et al. (1967). Scaling of experimental data in cerebral concussion in subhuman primates to concussive threshold for man. *Proceedings in 11th Stapp Car Crash Conference.* Society of Automotive Engineers, New York, 47-52.

Ono, K., Kikuchi, A., Nakamura, M., Kobayashi, H. & Nakamura, N. (1980). Human head tolerance to sagittal impact reliable estimation deduced from experimental head injury

subhuman primates and human cadaver skull. *Proceedings in the 24th Stapp Car Crash Conference,* SAE Paper No. 801303.

Padgaonkar, A.J., Krieger, K.W. & King, A.I. (1975). Measurement of angular acceleration of a rigid body using linear accelerometers. *Journal of Applied Mechanics, 42*(3), 552-556.

Pellman, E.J., Viano, D.C., Tucker, A.M. & Casson, I.R. (2003). Concussion in professional football: location and direction of helmet impacts – Part 2. *Neurosurgery, 53*, 1328-1341.

Pellman, E.J., Viano, D.C., Withnall, C. & Shewchenko, N. (2006). Concussion in professional football: helmet testing to assess impact performance – part 11. *Neurosurgery, 58*, 78-95.

Post, A., Gimbel, G. & Hoshizaki, T.B. (2011, May). The influence of headform geometry and headform mass on alpine ski helmet performance. *Journal of ASTM* International, 9(4).

Post, A., Hoshizaki, T.B. & Gilchrist, M.D. (2010). Finite element analysis of the effect of loading curve shape on brain injury predictors. *Journal of Biomechanics, 45*(4), 679-683.

Post, A., Oeur, A., Hoshizaki, B. & Gilchrist, M.D. (2011). Examination of the relationship between peak linear and angular accelerations to the brain deformation metrics in hockey helmet impacts. *Computer Methods in Biomechanics and Biomedical Engineering,* 1-9.

Pudenz, R.H. & Shelden, C.H. (1946). The Lucite calvarium-a method for direct observation of the brain; cranial trauma and brain movement. *Journal of Neurosurgery, 3*, 487-505.

Robertson, D.G.E. (2008). *Bioproc 2 Data Processing System*. Ottawa, ON, University of Ottawa.

Robertson, D.G.E. (1997). *Introduction to Biomechanics for Human Motion Analysis (2nd ed*.) Waterloo, ON, Waterloo Biomechanics.

Roe, C., Sveen, U., Alvsaker, K. & Bautz-Holter, E. (2009). Post-concussion symptoms after mild traumatic brain injury: Influence of demographic factors and injury severity in a 1-year cohort study. *Disability and Rehabilitation, 31*(15), 1235-1243.

Rousseau, P., Post, A. & Hoshizaki, T.B. (2009). A comparison of peak linear and angular headform accelerations using ice hockey helmets. *Journal of ASTM International, 6*(1).

Ruan, J. (1994). Impact biomechanics of head injury by mathematical modeling, PhD thesis, Wayne State University.

Ruan, J.S., Khalil, T.B. & King, A.I. (1993). Finite element modeling of direct head impact. *Proceedings of the 37th Stapp Car Crash Conference*, San Antonio, Texas, USA, SAE 933114.

Ryan, L.M. & Warden, D.L. (2003). Post concussion syndrome. *International Review of Psychiatry, 15*(4), 310-316.

Shewchenko, N., Withnall, C., Keown, M., Gittens, R. & Dvorak, J. (2005). Heading in football. Part 3: Effect of ball properties on head response. *British Journal of Sports Medicine, 39*, 33-39.

Schnebel, B., Gwin, J.T., Anderson, S., et al. (2007). In vivo study of head impacts in football: a comparison of National Collegiate Athletic Association Division I versus high school impacts. *Journal of Neurosurgery, 60*, 490–495.

Sigurdardottir, S., Andelic, N., Roe, C., Jerstad, T. & Schanke, A.K. (2009). Post-concussion symptoms after traumatic brain injury at 3 and 12 months post-injury: A prospective study. *Brain Injury, 23*(6), 489-497.

Silva, V.D. (2006). *Mechanics and Strength of Materials*. New York, NY, Springer Berlin Heidelberg.

Smith, P.K. & Hamill, J. (1986). The effect of punching glove type and skill level on momentum transfer. *Journal of Human Movement Studies, 12*, 135-161.

Snell Memorial Foundation (2000). 1995 Standard for Protective Equipment, 1998 Revision. For use in Bicycling. North Highlands, CA.

Society of Automotive Engineers International. (2007). Instrumentation for Impact Test – Part 1 – Electronic Instrumentation. *Surface Vehicle Recommended Practice*, J211-1.

SPSS Inc. (2010). *SPSS Base 18.0 for Windows User's Guide*. SPSS Inc., Chicago IL.

Strich, S. (1961). Shearing of nerve fibers as a cause of brain damage due to head injury. *Lancet, 2*, 443-448.

Trosseile, X., Tarriere, C., Lavaste, F., Guillon, F. & Domont, A. (1992). Development of a F.E.M. of the human head according to a specific test protocol. *Proceedings of 36th Stapp Car Crash Conference, SAE Paper No. 922527*.

Unterharnscheidt, F.J. & Higgins, L.S. (1969). Traumatic lesions of brain and spinal cord due to nondeforming angular acceleration of the head. *Texas Reports on Biology & Medicine. 27*, 127-166.

Viano, D.C., Casson, I.R., Pellman, E.J., Bir, C.A., Zhang, L., Sherman, D.C. & Boitano, M.A. (2005). Concussion in professional football : comparison with boxing head impacts—part 10. *Neurosurgery, 57*(6), 1154-1172.

Viano, D.C., King, A.I., Melvin, J.W. & Weber, K. (1989). Injury biomechanics research: an essential element in the prevention of trauma. *Journal of Biomechanics, 22*(5), 403-417.

Viano, D.C. & Pellman, E.J. (2005). Concussion in professional football: biomechanics of the striking player – part 8. *Neurosurgery, 56*, 266-280.

Versace, J. (1971). A review of the severity index.

Walilko, T.J., Viano, D.C. & Bir, C.A. (2005). Biomechanics of the head for Olympic boxer punches to the face. *British Journal of Sports Medicine, 39*, 710-719.

Walsh, E.S. & Hoshizaki, T.B. (2010). Sensitivity Analysis of a Hybrid III Head-and Neckform to Impact Angle Variation. *Proceedings in 8th Conference of the International Sports Engineering Association.*

Walsh, E.S., Rousseau, P. & Hoshizaki, T.B. (2011). The influence of impact location and angle on the dynamic impact response of a hybrid III headform. *Journal of Sports Engineering, 13*(3), 135-143.

Ward, C. & Thompson, R.B. (1975). The development of a detailed finite element brain model. *Proceedings of the 19th Stapp Car Crash Conference*, San Diego, California, USA, SAE 751163.

Willinger, R. & Baumgarthner. (2003). Human head tolerance limit to specific injury mechanisms. *International Journal of Crashworthiness, 8*(6), 605-617.

Willinger, R., Taled, L. & Kopp C. (1995). Modal and temporal analysis of head mathematical models. *Journal of Neurotrauma, 12,* 743-754.

Wood, R.L. (2004). Understanding the 'miserable minority': A diasthesis-stress paradigm for post-concussion syndrome. *Brain Injury, 18*(11), 1135-1153.

Yang, K.H. & King, A.I. (2003). A limited review of finite element models of development for brain injury biomechanics research. *International Journal of Vehicle Design, 31*(2), 116-130.

Zazryn, T., Cameron, P. & McCrory, P. (2006). A prospective cohort study of injury in amateur and professional boxing. *British Journal of Sports Medicine, 40*, 670-674.

Zhang, L., Yang, K.H. & King, A.I. (2001). Biomechanics of neurotrauma. *Neurological Research, 23*, 144-156.

Zhang, L., Yang, K.H., Dwarampudi, R., Omori, K., Li, T., Chang, K., Hardy, W.N., Khalil, T.B. & King, A.I. (2001). Recent advances in brain injury research: A new human head model development and validation. *Stapp Car Crash Journal, 45*, 369-393.

Zhang, L., Yang, K.H. & King, A.I. (2004). A proposed injury threshold for mild traumatic brain injury. *Journal of Biomechanical Engineering, 126*, 226-236

Zhang, L., Yang, K.H., King, A.I. & Viano, D.C. (2003) A new biomechanical predictor for mild traumatic brain injury – A preliminary report. *Summer Bioengineering Conference*, Key Biscayne, Florida.

Zhang, J., Yoganandan, N., Pintar, F.A. & Gennarelli, T.A. (2006a). Role of translational and rotational accelerations on brain strain in lateral head impact. *Biomedical Sciences Instrumentation, 42*, 501-506.

Zhang, J., Yoganandan, N., Pintar, F.A. & Gennarelli, T.A. (2006b). Brain strains in vehicle impact tests. *Annual Proceedings / Association for the Advancement of Automotive Medicine, 50*, 1-12.

Zhou, C. (1995). Finite element modeling of impact response of an inhomogeneous brain. Ph.D. Thesis, Wayne State University.

Zhou, C., Khalil, T. & King, A. (1996). A new model comparing impact responses of the homogeneous and inhomogeneous human brain. *Proceedings 39th Stapp Car Crash Conference*, San Diego, 121-137.

Zwahlen R.A., Labler, L., Trentz, O., Gratz, K.W. & Bachmann, L.M. (2007). Lateral impact in closed head injury: A substantially increased risk for diffuse axonal injury – A preliminary study. *Journal of Cranio-Maxillofacial Surgery, 35*, 142-146.

APPENDIX A: Side, top, and front visual representation of the centric and non-centric impact locations on a Hybrid III head form.

Centric → Side Center of Gravity

Non-Centric → Front Boss 45° Positive Azimuth

APPENDIX B: Dynamic response results for each impact trial across six inbound masses.

		Centric (Side CG)			Non-Centric (Front Boss PA)		
Inbound Mass (kg)	**Trial #**	**Velocity (m/s)**	**Linear Acc. (g)**	**Angular Acc. (rad/s^2)**	**Velocity (m/s)**	**Linear Acc. (g)**	**Angular Acc. (rad/s^2)**
4.3	1	3.92	177.7	15385	4.03	156.5	17605
	2	4.08	177.6	15406	4.01	155.3	18177
	3	4.12	178.6	15341	3.95	161.5	19192
	4	4.18	174.9	15439	3.78	151.3	19316
	5		180.1	14896	3.95	169.0	17924
Ave.		**4.08**	**177.8**	**15293**	**3.94**	**158.7**	**18443**
SD		0.11	1.9	225	0.10	6.8	769
6.3	1	4.17	202.8	16296	4.04	179.4	18802
	2	4.12	198.9	16017	3.93	176.5	19996
	3	4.08	199.7	15945	4.04	180.5	17997
	4	4.18	196.3	16424		179.5	18697
	5	4.12	199.1	15975	3.93	187.6	18549
Ave.		**4.13**	**199.4**	**16131**	**3.99**	**180.7**	**18808**
SD		0.04	2.3	215	0.06	4.1	733
8.3	1	4.14	210.8	17029	4.04	194.3	18434
	2	3.92	210.0	17062	3.93	189.8	18052
	3	4.09	209.8	16919	4.04	192.4	17648
	4	3.97	210.1	17166	4.04	190.4	17525
	5	3.83	211.7	17048	4.04	191.2	17257
Ave.		**3.99**	**210.5**	**17045**	**4.02**	**191.6**	**17783**
SD		0.13	0.8	88	0.05	1.8	463
10.3	1	4.02	219.9	17904	4.16	198.7	17810
	2	4.12	228.3	18141	4.04	198.2	19406
	3	4.08	236.4	17516	3.93	193.2	18343
	4	4.08	229.7	18264	4.16	195.8	17735
	5	3.98	227.8	18261	4.12	202.2	17806
Ave.		**4.06**	**228.4**	**18017**	**4.08**	**197.6**	**18220**
SD		0.06	5.9	316	0.10	3.4	706
12.3	1	4.18	223.3	17490	4.04	198.3	17702
	2	3.98	229.8	17958	4.16	204.6	18027
	3	4.18	230.9	17862	4.04	202.0	18342
	4	4.08	228.0	18014	3.93	194.7	18685
	5	4.08	230.1	18028	4.04	202.6	21156
Ave.		**4.10**	**228.4**	**17870**	**4.04**	**200.4**	**18782**
SD		0.08	3.1	222	0.08	3.9	1376
14.3	1	3.98	226.1	18622	4.01	227.1	20154
	2	3.98	232.0	17016	4.04	226.2	19989
	3	3.98	230.9	17216	4.12	227.1	19777
	4	3.88	231.3	17469	4.12	225.9	19974
	5	3.98	227.6	17313	4.01	226.4	19709
Ave.		**3.96**	**229.6**	**17527**	**4.05**	**226.5**	**19921**
SD		0.04	2.6	634	0.06	0.5	178

APPENDIX C: Brain tissue response results for each impact trial across six inbound masses.

		Centric (Side CG)			Non-Centric (Front Boss PA)		
Inbound Mass (kg)	**Trial #**	**Velocity (m/s)**	**Maximum principal strain**	**Von Mises stress (Pa)**	**Velocity (m/s)**	**Maximum principal strain**	**Von Mises stress (kPa)**
4.3	1	3.92	0.284	10374	4.03	0.490	19536
	2	4.08	0.287	10211	4.01	0.512	20459
	3	4.12	0.280	9864	3.95	0.506	20107
	4	4.18	0.276	9529	3.78	0.525	21038
	5		0.300	10451	3.95	0.462	18289
Ave.		**4.08**	**0.285**	**10086**	**3.94**	**0.499**	**19886**
SD		0.11	0.009	384	0.10	0.024	1046
6.3	1	4.17	0.302	10733	4.04	0.528	21069
	2	4.12	0.304	11188	3.93	0.561	22425
	3	4.08	0.299	10941	4.04	0.523	20645
	4	4.18	0.304	11246		0.547	21717
	5	4.12	0.311	11160	3.93	0.523	20571
Ave.		**4.13**	**0.304**	**11054**	**3.99**	**0.536**	**21285**
SD		0.04	0.004	213	0.06	0.017	783
8.3	1	4.14	0.324	11473	4.04	0.501	19721
	2	3.92	0.319	11335	3.93	0.519	20376
	3	4.09	0.309	11045	4.04	0.488	18993
	4	3.97	0.320	11471	4.04	0.476	18644
	5	3.83	0.303	10946	4.04	0.481	18629
Ave.		**3.99**	**0.315**	**11254**	**4.02**	**0.493**	**19273**
SD		0.13	0.009	245	0.05	0.017	759
10.3	1	4.02	0.306	11828	4.16	0.516	20053
	2	4.12	0.347	12504	4.04	0.533	21063
	3	4.08	0.322	11752	3.93	0.544	21415
	4	4.08	0.335	12184	4.16	0.527	20522
	5	3.98	0.339	12519	4.12	0.515	20018
Ave.		**4.06**	**0.330**	**12157**	**4.08**	**0.527**	**20614**
SD		0.06	0.016	362	0.10	0.012	617
12.3	1	4.18	0.298	11814	4.04	0.534	20799
	2	3.98	0.330	11825	4.16	0.534	20717
	3	4.18	0.332	12206	4.04	0.544	21165
	4	4.08	0.337	12397	3.93	0.566	22323
	5	4.08	0.332	12152	4.04	0.633	25446
Ave.		**4.10**	**0.326**	**12079**	**4.04**	**0.562**	**22090**
SD		0.08	0.016	254	0.08	0.042	1983
14.3	1	3.98	0.329	12494	4.01	0.506	19434
	2	3.98	0.320	11372	4.04	0.535	20715
	3	3.98	0.326	11590	4.12	0.528	20328
	4	3.88	0.312	11086	4.12	0.516	19865
	5	3.98	0.337	11964	4.01	0.494	18927
Ave.		**3.96**	**0.325**	**11701**	**4.05**	**0.516**	**19854**
SD		0.04	0.009	547	0.06	0.016	707

APPENDIX D: Percent difference between centric and non-centric impacts for each dependent variables across six inbound masses.

	Percentage Difference (%)			
Inbound Mass (kg)	**Linear Acc.**	**Angular Acc.**	**Maximum principal strain**	**Von Mises stress**
4.3	11.3	18.7	54.5	65.4
6.3	9.8	15.3	55.3	63.3
8.3	9.4	4.2	44.1	52.5
10.3	14.5	1.1	46.0	51.6
12.3	13.0	5.0	53.2	58.6
14.3	1.3	12.8	45.4	51.7